Soft Matter

REVIEW

View Article Online
View Journal | View Issue

Published on 25 April 2014. Downloaded by Michigan State University on 24/01/2016 09:49:48.

Cite this: *Soft Matter*, 2014, **10**, 5428

Gelation induced supramolecular chirality: chirality transfer, amplification and application

Pengfei Duan,† Hai Cao,‡ Li Zhang and Minghua Liu*

Received 5th March 2014
Accepted 25th April 2014

DOI: 10.1039/c4sm00507d

www.rsc.org/softmatter

Supramolecular chirality defines chirality at the supramolecular level, and is generated from the spatial arrangement of component molecules assembling through non-covalent interactions such as hydrogen bonding, van der Waals interactions, π–π stacking, hydrophobic interactions and so on. During the formation of low molecular weight gels (LMWGs), one kind of fascinating soft material, one frequently encounters the phenomenon of chirality as well as chiral nanostructures, either from chiral gelators or even achiral gelators. A view of gelation-induced supramolecular chirality will be very helpful to understand the self-assembly process of the gelator molecules as well as the chiral structures, the regulation of the chirality in the gels and the development of the "smart" chiral materials such as chiroptical devices, catalysts and chiral sensors. It necessitates fundamental understanding of chirality transfer and amplification in these supramolecular systems. In this review, recent progress in gelation-induced supramolecular chirality is discussed.

1. Introduction

Chirality is one of the fundamental properties found in nature. It is inherent in biological systems and essential to the functioning of sophisticated biological activities that occur in living systems. Chirality displays itself in diverse forms and occurs at various hierarchical scales from molecular, macromolecular, and supramolecular levels to nano-/macroscopical level.[1–6]

Supramolecular chirality describes the chirality of the supramolecular regimes based on non-covalent interactions such as hydrogen bonding, van der Waals interactions, π–π stacking, hydrophobic interactions and so on. It is related not only to the chirality of the molecules, but is also largely dependent on the spatial arrangements or the assembly manner of the component molecules. While the origin of homochirality in nature is still unresolved, great effort has been devoted to the design and application of chiral molecules and supramolecular chiral systems in recent years. In particular, supramolecular chirality *via* the principles of a supramolecular approach has become a current interesting interdisciplinary field of

Key Laboratory of Colloid, Interface and Chemical Thermodynamics, Institute of Chemistry, The Chinese Academy of Sciences, Beijing, 100080, People's Republic of China. E-mail: liumh@iccas.ac.cn; Fax: +86-10-62569564; Tel: +86-10-62569563

† Present address: Center for Molecular Systems (CMS), Kyushu University, 744 Moto-oka, Nishi-ku, Fukuoka 819-0395, Japan.

‡ Present address: Division of Molecular Imaging and Photonics, Department of Chemistry, KU Leuven, Celestijnenlaan 200 FB-3001, Leuven, Belgium.

Pengfei Duan is an assistant professor at Kyushu University, Japan. He received his PhD in physical chemistry from the Institute of Chemistry, Chinese Academy of Sciences (CAS) in 2011 with Prof. Minghua Liu. He focuses on the development of novel molecular gelators and defining the relationship between molecular chirality and supramolecular chirality. His research interests include supramolecular chirality, chiral structures, photochemistry and photon-upconversion.

Hai Cao completed his PhD in physical chemistry in 2012 with Prof. Minghua Liu at the Institute of Chemistry, Chinese Academy of Sciences (CAS). His PhD work was about the fabrication and application of chiral nanostructures based on amino acid derivatives. He is now a postdoc at KU Leuven in Belgium. His research interests cover supramolecular chirality in Langmuir and Langmuir–Blodgett films, self-assembled gels, colloids and chiral nanomaterials.

This journal is © The Royal Society of Chemistry 2014

Published on 25 April 2014. Downloaded by Michigan State University on 24/01/2016 09:49:48.

research.[7–13] During such a process, an important issue is how molecular chirality could be transferred to the supramolecular level.

Among various self-assembled systems, supramolecular gels, including low-molecular-weight organogels (LMWGs) and hydrogels, are fascinating soft materials.[14–19] It is interesting that many gelators are chiral molecules and thus the supramolecular gel system provides a large library to investigate supramolecular chirality. Starting from either chiral or achiral molecules, the intermolecular interactions may possibly lead to the formation of chiral aggregates in the gels. Such properties can be characterized by a series of methods such as CD spectroscopy, AFM, SEM and TEM. Since supramolecular chirality is pretty sensitive to the molecular alignment of multicomponent assembly, its implications are comprehensive for a broad range of molecular sciences. This intriguing phenomenon is widely seen in nature and various artificial and biomimetic systems, which offers the opportunity to control the properties of materials in a dynamic and reversible manner.

Generally, gelator molecules can self-assemble into fibers, tapes, strands, or other aggregations with high aspect ratios through non-covalent bonds, depending on their molecular structures and their interaction with the solvent molecules.[15,17,18] These elongated objects entangle each other to form three-dimensional networks that can immobilize solvents by capillary forces and surface tension. When the gelator molecules are chiral, these nanostructures can be endowed with chiral characteristics, such as chiral twist, chiral tube and so on. Thus, the supramolecular chirality can be directly visualized using AFM, SEM and TEM. In addition, the responsive nature of the gel, which could be easily tuned by the pH, photo-irradiation, ultrasound, heat and so on, provides chances to regulate the chirality in the gel system. Thus, supramolecular gels could serve as a good example to understand the emergence, transfer, amplification and functionalization of chirality in supramolecular systems.

In this review, we want to focus on recent developments of gelation-induced supramolecular chirality based on LMWGs. We will try to summarize some general concepts in this field with the hope of shedding some light on future work. The following content will be included in this review: (i) chirality transfer in gel systems; (ii) expression of supramolecular chirality at the nano/micro scale from LMWGs; (iii) application of gelation-induced supramolecular chirality.

One of the significant advantages of gelation-induced supramolecular chirality is that it can effectively deliver molecular packing information in LMW gels. In supramolecular systems, chirality transfer can occur in three cases. In the case of a gel system purely composed of chiral gelators, the chirality can be transferred from molecules to the self-assembled aggregates through non-covalent bonds. In the mixed system of a chiral gelator with an achiral dopant, co-assembly though non-covalent interactions leads to the transfer of chirality. When it comes to the gels formed by achiral building blocks, symmetry breaking during the gelation process results in the formation of chiral aggregates with undetermined handedness. Thus, gelation-induced supramolecular chirality can be divided into three types according to the pattern of chirality transfer: (i) induced supramolecular chirality in chiral gel systems (Scheme 1a); (ii) induced supramolecular chirality of achiral compounds

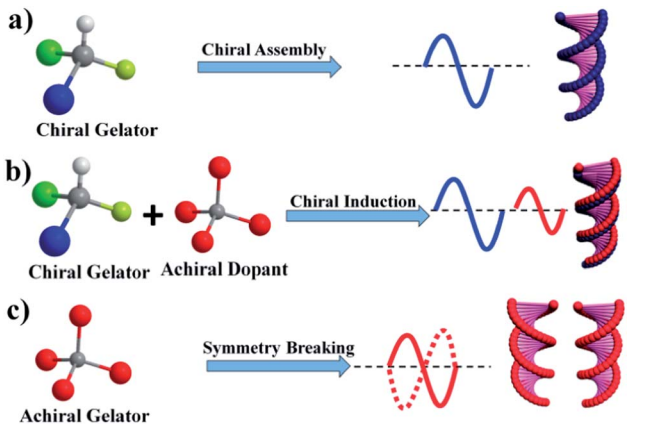

Scheme 1 Classification of gelation-induced supramolecular chirality. Chiral assemblies from (a) exclusively chiral gelator molecules, (b) the combination of chiral and achiral molecules. (c) exclusively achiral gelator molecules.

Li Zhang received her PhD in physical chemistry from the Institute of Chemistry, Chinese Academy of Sciences in 2004. She is currently an associate professor at the Institute of Chemistry, CAS. Her research interest is supramolecular chirality in supramolecular gels.

Minghua Liu graduated from Nanjing University in 1986 and received his PhD from Saitama University in 1994. He has been working on colloid and interface science, supramolecular chemistry and soft materials. He is currently a professor at the Institute of Chemistry, Chinese Academy of Sciences. His research interests cover supramolecular chirality in Langmuir and Langmuir–Blodgett films, self-assembled gels, colloids and chiral nanomaterials.

Published on 25 April 2014. Downloaded by Michigan State University on 24/01/2016 09:49:48.

in chiral gel systems (Scheme 1b); (iii) symmetry breaking in achiral gel systems (Scheme 1c). In the following section, we will discuss these typical supramolecular chirality using some representative examples.

2. Gelation-induced supramolecular chirality

2.1 Supramolecular chirality in gel systems composed of a chiral gelator

Although most new gelator families are still being discovered by serendipity, the design of the gelator is becoming easier. The induction of the chiral centre is frequently adopted. Molecular chirality is supposed to play an important role in the formation of supramolecular gels, which has been frequently reported.[15] One generally accepted mechanism of induced supramolecular chirality in chiral gel system is that, in the gelation process, chirality can be transferred from gelator molecules to the self-assembled aggregates. In the presence of a chromophore, there will be an exciton and the alignment of chiral molecules to induce a signal observable in the CD spectrum. However, in the solution state, no CD signal could be detected. This means that in solution or in a free state, the chirality of the chiral centre that is far from the chromophore cannot be transferred to the chromophore. Thus, the supramolecular chirality is induced by the gel formation process. It strongly relates to the physical state of the chiral gels. In other words, gelation-induced supramolecular chirality of a chiral gel is quite sensitive to the gel–sol transformation regulated by external multiple stimuli. This intriguing property will be summarized in an individual section. Transfer of chirality from chiral gelators to assembled aggregates has a close relationship with the molecular structure of the chiral gelators. Generally, the spacer length and spacer group influence the chirality transfer. We have selected some examples that are illustrative to give a clear perspective in this section. Additionally, gelation solvent-mediated chirality inversion, as an intriguing research issue, has received increased attention in recent years. We will also summarize it as an individual section.

2.1.1 Transfer of chiral information from chiral centre to chromophore

A series of L-glutamate-based dendrons containing aromatic groups, including phenyl (**1a**), naphthyl (**1b**, **1c**) and anthryl (**1d**), were found to form organogels in hexane or hydrogels, as shown in Fig. 1.[20] The hydrogen bonds between the amide groups and the π–π stacking between the aromatic rings are the main driving forces for the self-assembly of glutamate dendrons in organic solvents and water. The glutamate dendrons gels showed distinct CD spectral patterns in accordance with their chromophores. However, no CD signals were detected from the THF solutions of corresponding dendrons, indicating that the CD signals observed in the supramolecular gels originated from the chiral aggregates of the gelators. Thus, we can easily conclude that transfer of chiral information from chiral centre to chromophore rather than intrinsic molecular chirality was

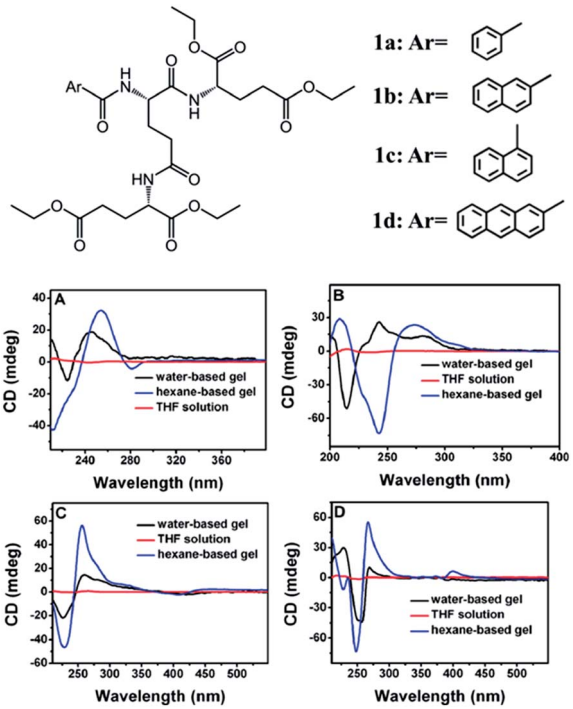

Fig. 1 Molecular structures of glutamate-based dendrons gelators **1a–d** and CD spectra of **1a** (A), **1b** (B), **1c** (C), and **1d** (D) in THF solution (red), a water-based gel phase (black), and a hexane-based gel phase (blue). Reprinted with permission from ref. 20. Copyright (2009) American Chemical Society.

responsible for the emergence of the CD signals. The transfer of chirality also occurred in the supramolecular gels of L-glutamate-based dendrons induced by ultrasonication. The supramolecular chirality of chromophores in gels is supposed to derive from the chiral packing of chromophores induced by self-assembly of gelators. Unlike the free state of chromophores in solution, the chromophores are forced to pack in a confined space formed by the self-assembly of gelator through intermolecular non-covalent interactions. To decrease the energy, the chromophores are affected by the chirality of the chiral centre to show a chiral packing, similar to the results observed in liquid crystals[21] and LB films.[22]

However, the transfer of chirality from chiral centre to chromophore was strongly dependent on the intensity and types of intermolecular or intramolecular interactions. The Cotton effect of supramolecular chirality is in accordance with the intensity of chromophore interactions. Generally, strong intermolecular interaction will be favourable for the transfer, especially strong H-bonding and π–π stacking. Split and intense CD signals can be obtained when strong inter-chromophore stacking is adopted in gel system. However, one more acceptable description is that the induced chirality is the result of the synergy between various non-covalent interactions. As shown in Fig. 2, three isomeric pyridine-containing L-glutamic lipids formed organogels in DMSO and self-assembled into different nanostructures of nanofiber, nanotwist and nanotube depending on the substituent position in the pyridine ring.[23]

 This journal is © The Royal Society of Chemistry 2014

Published on 25 April 2014. Downloaded by Michigan State University on 24/01/2016 09:49:48.

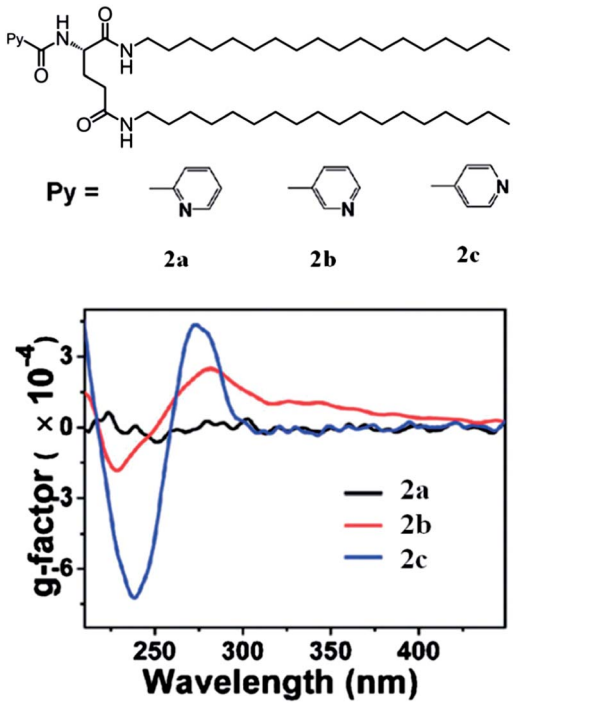

Fig. 2 Molecular structures of pyridine-bearing chiral lipid gelators **2a–c** and relative CD spectra of corresponding DMSO gels. Adapted from ref. 23.

Clearly, the three isomers have the same chiral centre in the glutamate segment. However, the induced chirality expressed in the CD spectra is different. Due to the strong hydrogen bonds of the amide groups, π–π stacking of pyridyl and the hydrophobic interaction of alkyl chains, the glutamate chirality of **2c** can be transferred to the pyridyl aggregate and expressed as supramolecular chirality in the CD spectrum with a strong Cotton effect. **2b** has relatively weak intermolecular interactions, which resulted in a weaker CD signal. In the case of **2a**, the intramolecular hydrogen bonds weakened the packing between the molecules and thus **2a** only assembled into nanofibers. In addition, the chirality of the L-glutamic acid was not transferred to the pyridyl ring due to a lack of strong π–π packing between the pyridyl rings. It is obvious that even though the three isomers have the same chiral centre, the results of gelation-induced supramolecular chirality can be different. The synergy of intermolecular interactions should be highlighted in the process of chirality transfer. It is clear that in the process of chirality transfer in a chiral gel system, intermolecular non-covalent bonds are a crucial factor. A slight change in molecular structure may affect the situation as a whole in chirality transfer.

The hydrophobic chain length has been found to affect the transfer and expression of chirality in gels. Cui *et al.* elucidated the effect of terminal chain length on the chiral expression ability of the gels formed by a series of sugar-appended organogelators, 4-(40-alkoxyphenyl)phenyl-β-*O*-D-glucoside (GBC*n*, where $n = 1$–12 denotes the number of carbon atoms in the tail). They found that the gels formed by GBC*n* (n = 3–6, 11, 12) exhibited intensive Cotton effects in the absorption region of the biphenyl group, while the GBC*n* (n = 7–10) that cannot generate gels only showed negligible signals, which implied an intrinsic relationship between chiral expression and the gel formation.[24]

Another example of gelator molecular structures influencing chirality transfer is the even–odd effect.[25] We have investigated a series of bola-form gelators with different alkyl chain lengths. Similar to the result that the odd and even numbers of CH_2 in the alkyl chain spacer could affect the gel formation, gelation-induced supramolecular chirality in chiral gels also showed dependence on the even–odd effect. As shown in Fig. 3, after gelation, a bola-form gelator with an odd number of methylene units (**3b**) showed a totally different CD spectrum to the gelator with an even number methylene units (**3a**), even in the same solvent. It is understandable that in the gelation, the structural characteristics of the linkers, including the phenyl groups and the length of alkyl chains, play important roles. However, the even–odd effect might be the main reason leading to different chirality transfer by influencing the intermolecular hydrogen bond formation and π–π stacking.

2.1.2 Chirality inversion

In supramolecular chiral systems, chirality inversion is particularly interesting, since switching between different supramolecular chiral states could, in principle, have potential applications in data storage, optical devices, and chromatographic chiral separation. Moreover, stable chiral aggregates with favourable photophysical properties that exhibit reversible switching between *P* and *M* supramolecular assemblies could have applications as chiroptical materials. *P*–*M* transition

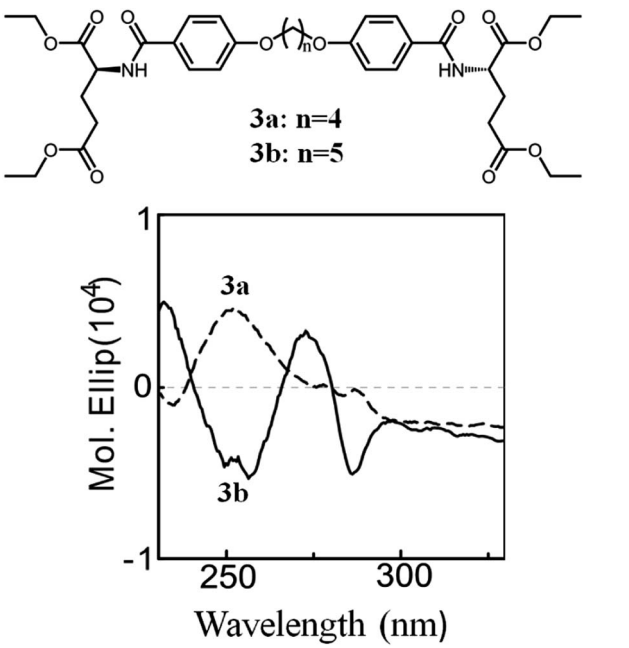

Fig. 3 Molecular structures of **3a** and **3b** and corresponding CD spectra during gelation in water–methanol (0.2 wt%, water–methanol = 3/10). Adapted from ref. 25.

Published on 25 April 2014. Downloaded by Michigan State University on 24/01/2016 09:49:48.

driven by external stimuli has already been reported in synthetic helical polymers.[26,27] Recently, some researchers have explored chirality inversion in supramolecular assemblies concerning various amphiphiles. Some work has been reviewed in important literature on the topic of chirality.[6] This section is compressed so as to limit overlap with previous reviews. It extends the field covered to gelation-induced chirality inversion in chiral gel systems.

In chiral gel systems, gelation-induced supramolecular chirality is sensitive to gelling solvents. The induced chirality expressed in CD spectra is related to the chromophore packing model. Meanwhile, solvent–gelator interactions profoundly affect the stability of conformationally flexible molecules and their higher-ordered assemblies. Our group has reported a glutamate based lipid gelator bearing an azobenzene segment which showed an excellent photoregulated gel–sol transition.[28] More interestingly, totally opposite CD signals were observed in DMSO and toluene gels: the DMSO gel exhibits a positive Cotton effect while a negative Cotton effect is observed in the toluene gel, as shown in Fig. 4. Actually, the induced supramolecular chirality showed the same phenomenon in other solvents: a positive Cotton effect was exhibited in polar solvents, while a negative Cotton effect was observed in nonpolar solvents. The induced supramolecular chirality was confirmed by monitoring the CD spectra of the xerogel cast film. The obtained CD spectra of the xerogel retain the same peak shape as the gel states, which reveals that the CD spectra of the gel states are authentic. The opposite Cotton effect obtained from different solvents implies that the reversed supramolecular chirality results from different molecular orientation at the molecular level. According to the results of XRD and temperature-dependent UV-vis spectra, two kinds of molecular stacking models were proposed: (a) the azobenzene groups packed face to face (π–π stacking); (b) the amino acids packed by forming H-bonds, as shown in Fig. 4A. This result was confirmed by density functional theory (DFT) calculations. The calculated CD spectra are considered to be in satisfactory agreement with the observed spectra of the gels. Moreover, the inversion of the CD signal in polar and nonpolar solvents observed here might contribute to a better understanding of similar systems.[29]

Xue, Ihara and co-workers have reported a glutamate derivative organogelator functionalized by phenylenevinylene units, which showed remarkable chiral inversion in mixed solvents based on DMSO and other organic solvents,[30] as shown in Fig. 5. Very interestingly, when adjusting the ratio of DMSO to diphenyl ether from 10 : 0 to 1 : 9, the absorption and CD spectra of **5** showed dynamic conversion. Two aggregation types with different packing systems existed in the mixed solvent system. As mentioned above, the polarity of the gelling solvent is related to the molecular packing model. However, in this case, it was confirmed that solvent polarity had no effect on the conversion proportion of the molecular packing. The induced supramolecular chirality inversion is the result of the solubility of the gelator molecules in mixed solvent systems. This can be confirmed by the aggregation behaviour from absorption spectra: a large scale blueshift indicated the strong packing of chromophores, which led to chirality inversion.

Wan and co-workers have reported a sugar based organogelator **6**, which showed gelation ability in mixed solvents.[31] More interestingly, gels of **6** show chirality inversion by different cooling speeds. As shown in Fig. 6A, **6** was CD silent in the solution state while a positive signal was observed in the slow-cooled gel and a negative signal was observed in the fast-cooled gel. Meanwhile, the fast-cooling process yielded right-handed helical ribbons, while the slow-cooling process yielded the left-handed counterparts. The author concluded that the formation of right-handed helical ribbons is kinetically favoured, and that of left-handed helical ribbons is thermodynamically favoured. Detailed experiments confirmed that the induced

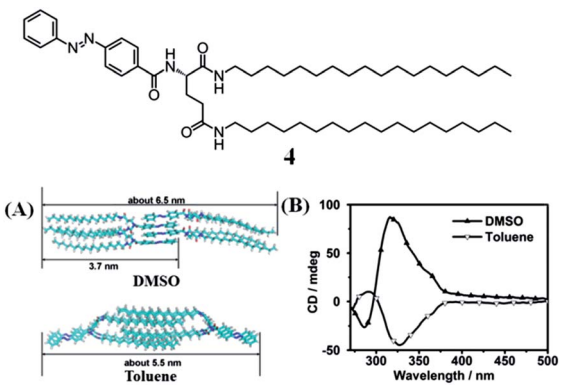

Fig. 4 Molecular structure of the azobenzene derivative **4**. (A) Scheme illustration of molecular packing in DMSO and toluene. (B) CD spectra of gel **4** in various states: DMSO gel (▲) with a concentration of 4.3 mM, and toluene gel (▽) with a concentration of 5.0 mM. Reprinted with permission from ref. 28. Copyright (2011) American Chemical Society.

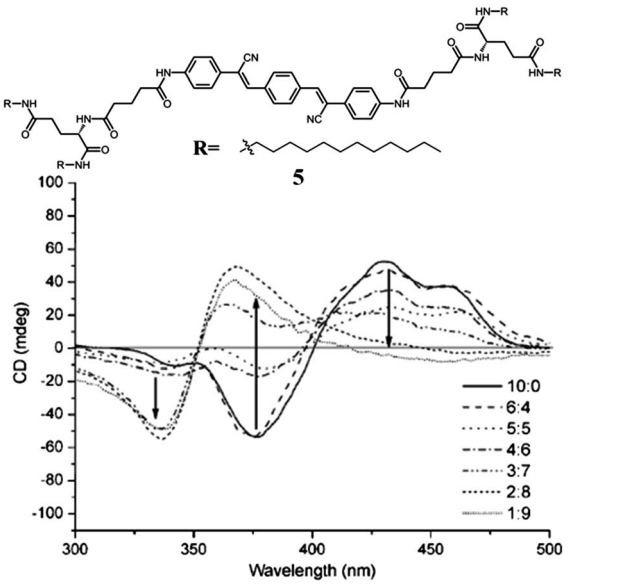

Fig. 5 Molecular structure of the lipid gelator **5** and CD spectra of the gelator in DMSO–diphenyl ether in variable ratios of DMSO and diphenyl ether. Reprinted with permission from ref. 30. Copyright (2009) John Wiley and Sons.

This journal is © The Royal Society of Chemistry 2014

Published on 25 April 2014. Downloaded by Michigan State University on 24/01/2016 09:49:48.

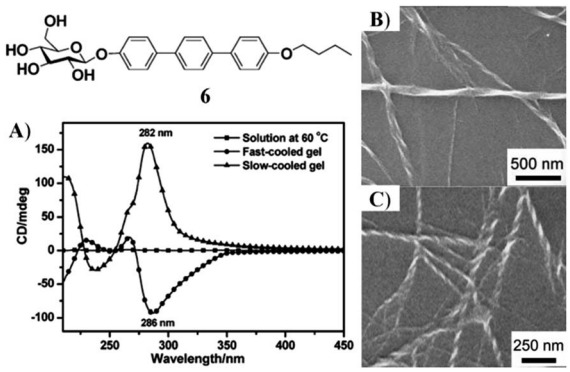

Fig. 6 Sugar based gelator molecular structure **6** and (A) CD spectra of **6** in H_2O–1,4-dioxane (40/60 v/v) with a concentration of 2 mg mL^{-1} in the solution state at 60 °C (■), fast-cooled gel state (●), and slow-cooled gel state (▲) at 20 °C. SEM images of the gels of **6** obtained through the slow-cooling process (B), and the fast-cooling process (C). Reprinted with permission from ref. 31. Copyright (2010) American Chemical Society.

supramolecular chirality was dependent on cooling rate. Moreover, the fast-cooling gel is metastable while the slow-cooling gel is stable. In the fast cooling process, the metastable nuclei would directly grow into right-handed ribbons, while in the slow-cooling process, the metastable nuclei evolved into stable nuclei and then further aggregated to form left-handed ribbons. In the gel state, the right-handed ribbons could not evolve to left-handed ribbons due to the kinetically controlled network structures. Consequently, the right-handed ribbons were obtained *via* kinetically controlled process, while the left-handed ribbons were obtained *via* a thermodynamically controlled process.

2.2 Chirality transfer from chiral molecules to achiral molecules in a binary gel

It is well known that at the supramolecular level, chirality is strongly related to the molecular assembly and that all kinds of molecules, either chiral or achiral, can be assembled into chiral assemblies through non-covalent bonds. One of the greatest merits of the supramolecular system is that achiral molecules can be induced into chiral self-assemblies, which opens up great possibilities for the design and fabrication of functional chiral materials.[32,33] Generally, chirality transfer in achiral and chiral hybrid system concerns two different situations depending on the ratio of achiral/chiral molecules. (i) Co-assembly of chiral and achiral molecules leads to the formation of new chiral aggregates. (ii) A small amount of chiral component induces achiral or racemic self-assembled systems into supramolecular chiral aggregates, following the 'sergeants and soldiers principle' and 'majority rules'. The basic characteristics and general phenomenon of induced-supramolecular chirality of chiral and achiral hybrid gel systems will be discussed for both of these cases.

2.2.1 Chirality transfer from chiral gelator to achiral dopant

Chirality transfer from a chiral compound to an achiral compound is an important mechanism by which chiral 'information' can be amplified by another achiral system. It is suggested that amplification of chirality is a key step in the origin of biomolecular homochirality during the evolution of life. In supramolecular chemistry, chiral induction is also an attractive issue. Especially in the supramolecular gel field, plenty of literature has reported on this subject. Most of the reports are concerning 'two-component' gels: one chiral segment and another achiral compound form a co-gel through non-covalent interactions.[14,34] Molecular chirality can be transferred to achiral compounds after gelation and expressed as induced supramolecular chirality. Given the massive amount of literature that pertains to this subject, we do not intend to make an exhaustive presentation but have selected a small proportion of them, which is about the chiral induction of achiral dopants in chiral gel systems. Actually, the induced supramolecular chirality of an achiral dopant in a chiral gel system is the result of transfer and amplification of molecular chirality. There are several distinct characteristics of chirality transfer in these systems:

(i) Interaction between achiral dopant and chiral gelator is required. Moreover, this kind of interaction is neither too strong nor too weak. Under certain conditions, it is a balance of interaction. The gelation process will be broken if the interaction is too strong whereas molecular chirality cannot be transferred if the interaction is too weak.

(ii) There are three main interaction types in the chirality transfer model: hydrogen bonding, electrostatic interaction and alkyl chain interdigitation. Hydrogen bonding and electrostatic interaction are common and easy to achieve. Alkyl chain interdigitation is rarely reported because of the weaker interaction intensity.

(iii) The ratio of chiral gelator/achiral dopant is crucial for the co-gel formation as well as the chirality transfer.

Generally, the hydrogen bond, as one strong intermolecular interaction, is a common interactive model for chirality transfer.

Recently, we have reported one case of chirality transfer through hydrogen bonding in a chiral system.[35] As shown in Fig. 7, a simple supramolecular approach has been proposed to achieve chirality transcription and twisted nanostructures in a two-component system consisting of L-glutamic acid-based amphiphiles **7a**, **7b** and bipyridines **4Py**. A series of amphiphiles based on L-glutamic acid with saturated fatty acid chains of different lengths were designed. **7a** and **7b** can self-assemble into nanofibers in water, thus leading to hydrogels. Upon adding bipyridine to the system, the nanostructures underwent interesting changes due to the strong hydrogen bonding between the carboxylic acid and the pyridyl nitrogen atoms. The molecular chirality of gelator molecules can be transferred to the bipyridine aggregates by strong hydrogen bonding and is expressed as induced supramolecular chirality in the CD spectra. Additionally, the induced chirality is related to the host gelator molecular structure and the type of bipyridine.

Hydrogen bonding regulated chirality transfer in supramolecular gel systems has been reported in many other cases. However, alkyl chain-regulated chirality transfer is scarcely

Published on 25 April 2014. Downloaded by Michigan State University on 24/01/2016 09:49:48.

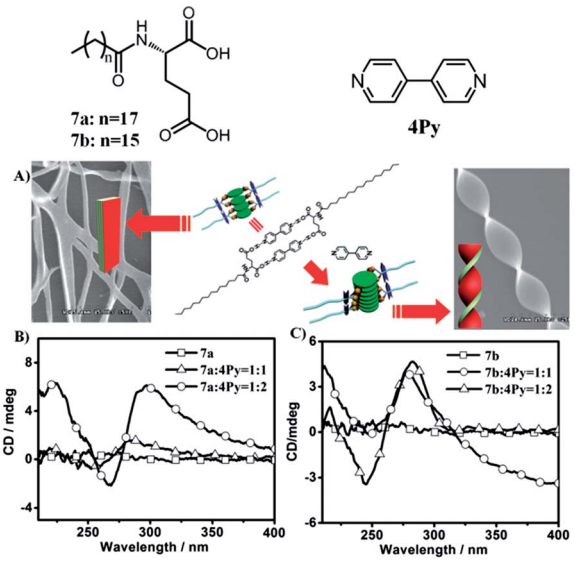

Fig. 7 Molecular structures of **7a**, **7b** and bipyridine (**4Py**); (A) schematic illustration and SEM images of co-assembled **7a**/**4Py** at different molar ratios; CD spectra of **7a**/**4Py** (B), **7b**/**4Py** (C) at different molar ratios. Reprinted with permission from ref. 35. Copyright (2011) John Wiley and Sons.

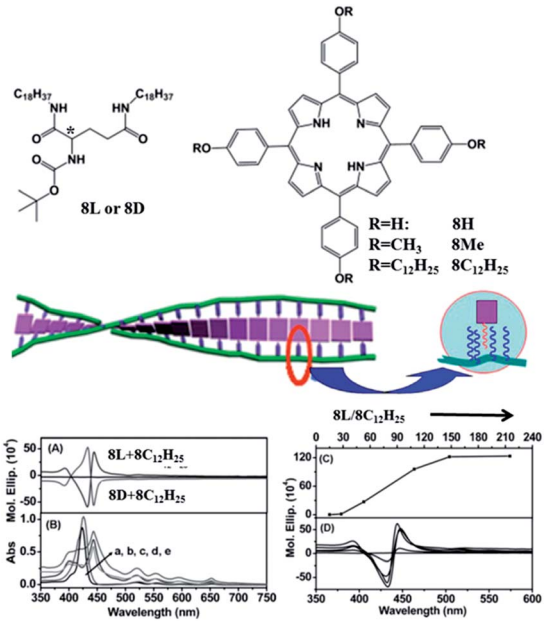

Fig. 8 Molecular structures of 8_L, 8_D, and dopant porphyrins and schematic illustration of their co-assembly. L and D refer to the chirality of the amino acid being used. CD spectra of $8C_{12}H_{25}$ mixed with 8_L, 8_D DMSO gel and that of $8C_{12}H_{25}$ DMSO solution. (B) (a) UV-vis spectra of $8C_{12}H_{25}$ solution in chloroform, (b) $8C_{12}H_{25}$ and 8_L in hot DMSO solution, (c) $8C_{12}H_{25}$ solution in DMSO at room temperature, (d) $8C_{12}H_{25}/8_L$, and (e) $8C_{12}H_{25}/8_D$ DMSO gel. (C) The plot of gelator/porphyrin ratio *versus* the intensity of the CD signals. (D) CD spectra of the $8C_{12}H_{25}/8_L$ DMSO gel at various gelator/porphyrin ratios. The concentration of gelators in all cases is 1.3×10^{-2} M. The concentration of porphyrin in (A) and (B) is 9×10^{-5} M, and is from 9.5×10^{-4} M to 6.5×10^{-5} M in (C) and (D). Adapted from ref. 39.

reported because of the relatively weaker interaction. Our group has developed several pioneering works concerning this concept.[36–40] We have reported one case concerning chiral induction in a chiral gel system.[39] Glutamate based chiral organogelators, 8_L and 8_D formed stable gels in DMSO. After doping with achiral porphyrin, a stable co-gel still could be obtained. Furthermore, a strong Cotton effect signal can be observed in the co-gels (Fig. 8). In this case, no structural similarity between the achiral porphyrin and chiral gelator exists except the alkyl chain. It revealed that the chirality of the gelator was transferred to the supramolecular assembly of the achiral porphyrin through the inter-chain interaction between the alkyl chains of both porphyrin and gelator during the gelation. It should be noted that when **8H** or **8Me**, which have no long alkyl chains, were applied in a similar way, CD signals were observed neither in mixed solutions nor in the organogel. This indicated that the long alkyl chain played an important role in chirality transfer. The gelator molecular chirality only can be transferred to porphyrin aggregates by inter-chain interactions. Meanwhile, the gelator/porphyrin ratio is also crucial to the chirality transfer, as shown in Fig. 8C and D. This implies that in the gel system about 150 times more chiral gelator molecules can completely control the aggregate direction of $8C_{12}H_{25}$ molecules. This ratio is much larger than the well-known 'sergeants and soldiers rule' systems in which the small amount of chiral sergeant molecules can direct the chiral orientation of numerous achiral soldier molecules. In this case, the situation is more like the achiral molecules doped in the chiral liquid crystals. The chiral three-dimensional environment provided by the chiral gelators and solvent molecules is suggested to be responsible for the induction of the chirality of $8C_{12}H_{25}$ assemblies.

Other non-covalent interactions, including electrostatic interactions and donor–acceptor interactions, have also been successfully utilized in inducing chirality in achiral dopants. Ihara *et al.* studied the self-assembly of a double long-chain alkylated L-glutamic acid as a molecular gelator.[41,42] The cationic pyridium moiety of the gelator can provided specific binding sites for achiral anionic guest molecules to induce secondary chirality, as shown in Fig. 9. Further, chirally-oriented lipid aggregates were doped into a solid polymer film, which was readily prepared by casting and removing a solvent from anionic L-glutamide-derived organogels and polystyrene. The induced CD signals can be detected in the polymer films due to chiral complex formation of the achiral dyes and the highly-ordered L-glutamide lipid structures based on electrostatic interactions.

2.2.2 Chirality transfer from trace chiral dopant to achiral gelator

Amplification of chirality occurs in systems in which a small initial amount of chiral bias induces a high diastereomeric or enantiomeric excess. Green and co-workers reported for the first time the amplification of chirality in polyisocyanates having a stiff helical backbone.[43,44] They found that polymers containing a small percentage of the chiral monomers still expressed a

 This journal is © The Royal Society of Chemistry 2014

Published on 25 April 2014. Downloaded by Michigan State University on 24/01/2016 09:49:48.

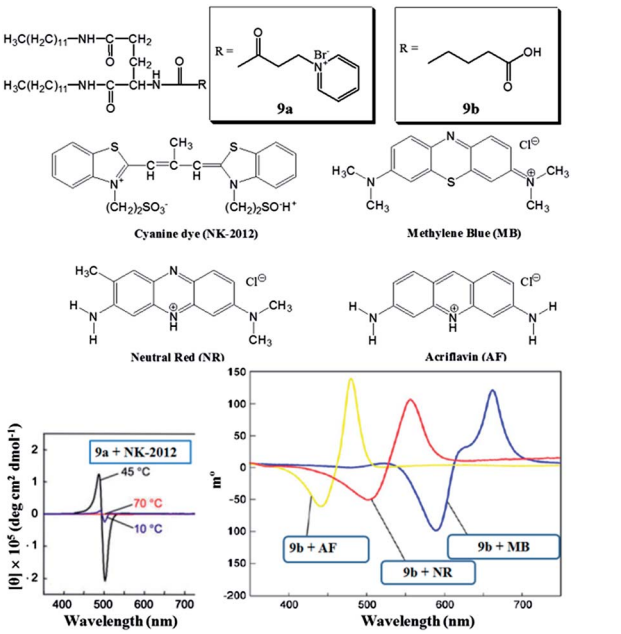

Fig. 9 Chemical structures of L-glutamic acid-based lipids **9a** and **9b** and various dyes used in the co-gel systems. Temperature dependent CD spectra of NK-2012 (0.01 mM) in the presence of **9a** (0.5 mM) in water and CD spectra of cationic dyes with **9b**-aggregates in polystyrene films. Reprinted with permission from ref. 41 Copyright (2007) Elsevier and ref. 42 Copyright (2010) Springer.

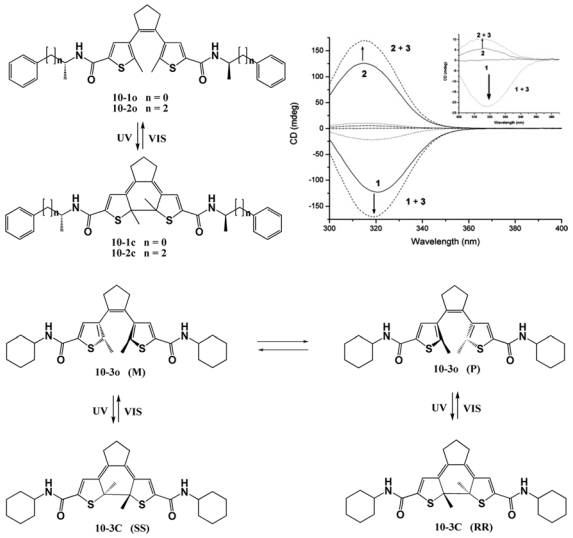

Fig. 10 System for chiral induction in gel-phase materials developed by van Esch, Feringa and co-workers. Chiral diarylethene switches **10** used for selection and amplification upon aggregation by hydrogen bond formation; (o) open form, (c) closed form, UV: $\lambda = 313$ nm, vis: $\lambda >$ 420 nm. CD spectrum of a 0.3 mM solution (inset) and 1.2 mM gel of 1° (—, negative CD signals) and a 0.3 mM solution (inset) and 1.3 mM gel of **10**–**2o** in toluene (—, positive CD signals). Upon addition of 1 equiv. of **10**–**3o** the signal increases (**- - -**, change is marked by arrows). Reprinted with permission from ref. 33. Copyright (2005) American Chemical Society.

strong chiroptical activity. The reason for this amplification is that the achiral units are forced to follow the helicity induced by the chiral units. This is commonly referred to as the 'sergeants and soldiers' principle. The 'sergeants and soldiers' principle describes the disproportionally large effect on optical activity of a small amount of chiral comonomer in a helical polymer of achiral monomers. It implies the control of the movements of large numbers of cooperative achiral units (the soldiers) by a few chiral units (the sergeants). This phenomenon has been proven to be applicable to supramolecular gel systems.[45,46]

Feringa, van Esch and co-workers reported a fascinating case in which they found it was possible to transfer chirality from one self-assembled system to another and then capture the transferred information in molecular form.[33] As shown in Fig. 10, the racemic gelator **10** has the potential to rapidly convert between *P* and *M* enantiomeric conformations after forming a racemic gel. Photochromic transformations can easily take place both in the solution and gel states accompanying the reversible spectral changes. Interestingly, the chirality of the gel phase was preserved during the photochromic reactions; moreover, the chirality was lost after gel–sol transition, and gels with opposite chirality were generated after further cooling the respective solutions. This gelator was then investigated in the presence of gelators **10-1** and **10-2**, which as well as interconverting between *P* and *M* forms, both contains two chiral centres. These auxiliary chiral centres mean that compound **10-1** prefers to assemble in the *P* form while gelator **10-2** prefers to assemble in the *M* form. Importantly, both gelator **10-1** and **10-2** are capable of co-assembly with gelator **10-3**. Even very small amounts of gelator **10-1** can induce gelator **10-3** to also assemble in the *P* form while gelator **10-2** can encourage gelator **10-3** to assemble in the *M* form. This was demonstrated by an increase in the CD signal associated with helical organisation of the dithienyl moiety. This indicates that gelator **10-1** or gelator **10-2** can transfer their chiral information to the assembly of gelator **10-3**, a principle referred to as 'sergeants and soldiers' assembly—a chiral 'sergeant' molecule is able to enforce its chiral preference onto a large number of achiral 'soldier' molecules.

2.3 Symmetry breaking in achiral gel system

In all the above cases, an intrinsically chiral component, either in enantiomeric excess or as a trace chiral trigger, is required for the induction and control of supramolecular chirality. However, at the supramolecular or macroscopic level chirality can also be realized on the exclusive basis of achiral molecules. To date induced supramolecular chirality, which is constructed from achiral molecules, has rarely been reported. However, in some particular cases, chiral assemblies can be obtained from pure achiral molecules. For instance, circular polarized light (CPL) or elliptically polarized light (EPL) can induce chirality in a system where no chiral inducer or dopant is present.[47] Some other examples are the spontaneous symmetry breaking in crystals and liquid crystals as well as some forms of dye aggregation in solution, whereby in both cases chiral supramolecular species are formed by achiral molecules.[48–52] Gelation-induced supramolecular chirality is of particular interest when it occurs in a totally achiral gel system. Construction of gelation-induced

Published on 25 April 2014. Downloaded by Michigan State University on 24/01/2016 09:49:48.

supramolecular chirality from achiral gelators will be paramount not only for developing the theory of chiral origin but also for further understanding many chirality-related self-assembly processes.

You and co-workers reported the first example describing chiral symmetry breaking in a gel state.[53] Fig. 11 shows a novel class of coordination polymer gelators, which only stem from the coordination of Ag(I) and the imidazole derivative **11b** or **11e**. The bridging organic ligands feature achirality, structural simplicity and a conformationally restricted bent shape. After gelation, a strong CD signal could be observed, which suggests the symmetry breaking happened during gel formation. The mirror symmetric CD signal indicated that the chirality was essentially governed by chance. It should be noted that this kind of induced supramolecular chirality is generated from symmetric breaking induced by strong directional interactions derived from the complex between the rigid bent bridging ligands and Ag(I), which adopts a linear coordination geometry.

3. Expression of supramolecular chirality at nano/micro scale

Research concerning the relationships between molecular, supramolecular and nanoscale chirality is very important in chiral science. Firstly, it is crucial for understanding various chiral structures in organisms; secondly, it is important to synthesize chiral nanostructures with precise controllability.

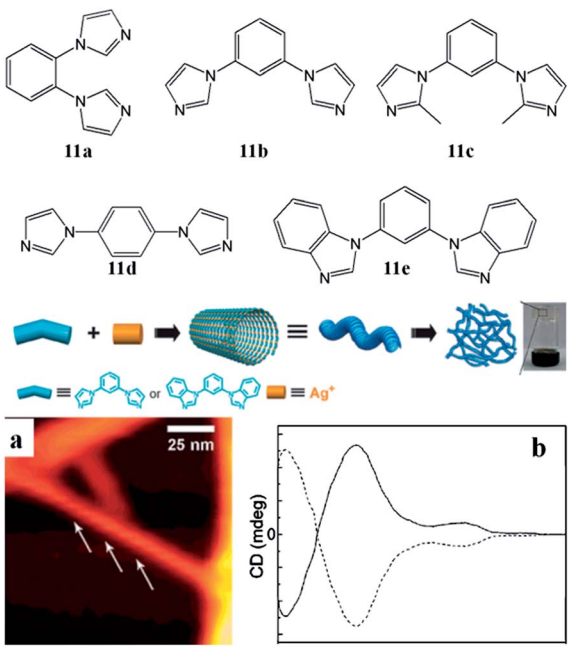

Fig. 11 Chemical structures and schematic representation of the self-assembly processes of the coordination polymer gels. Morphological and spectral analysis of the Ag–**11b** coordinated gel (0.8 wt%) in CH_3OH–H_2O. (a) AFM image of the gel. (b) CD spectra obtained for different batches, positive (positive to negative on going from longer to shorter wavelengths, solid line) or negative (dash line). Adapted from ref. 53.

Chirality effects in self-assembled fibrous networks have been reviewed in detail by Huc and Shinkai in different books.[15,54] Chiral assembly in gel systems is also covered. However, as an important issue in gelation-induced supramolecular chirality, expression at the nano/micro scale should be addressed. Here, we will consider some important subjects that are not described clearly in former reviews.

3.1 Molecular chirality and chiral nanostructures

As stated above, gelation-induced supramolecular chirality is obtained through chirality transfer in gel systems that are formed by chiral gelators or chiral–achiral hybrids. It is generally accepted that the expression of chiral self-assembly at the nanoscale results in chiral nanostructures. Nolte *et al.* gave us an ideal example from this point of view,[55,56] as shown in Fig. 12. Two disk-like molecules based on phthalocyanine with chiral and achiral side chains, respectively, can both form one dimensional nanostructures in chloroform. In both cases, these molecules self-assemble into long columnar aggregates, driven by π–π stacking interactions. However, the morphologies derived from chiral and achiral building blocks are obviously different. The strands of molecules **12a**, which have a diameter of about 6 nm, tend to align parallel to each other and nanofibers are formed. In the case of molecules **12b**, the strands of **12b** adopt a right-handed helical staggered packing, which further self-assemble into left-handed supercoils. Their experiments clearly describe the transfer and amplification of molecular chirality to supramolecular chirality, leading to the formation of chiral nanostructures.

Similar results have been widely reported ever since. In the case of chiral self-assemblies, another phenomenon has frequently been observed. The chiral nanostructures obtained from enantiomeric building blocks always appear with opposite handedness, as shown in Fig. 13. The glutamic acid based bolaamphiphile, **13b**$_L$, can form an organogel in a water–

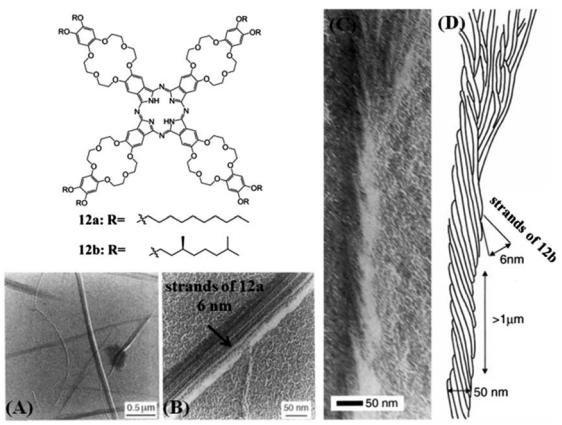

Fig. 12 Molecular structures of the phthalocyanine derivatives, **12a** and **12b**. (A and B) TEM images of the chloroform gel of **12a**. (C and D) TEM image and cartoon representation of the helices formed by **12b** in chloroform gel, respectively. Reprinted with permission from ref. 55 Copyright (1999) The American Association for the Advancement of Science.

This journal is © The Royal Society of Chemistry 2014

Published on 25 April 2014. Downloaded by Michigan State University on 24/01/2016 09:49:48.

ethanol mixture with the appearance of monolayered helical nanotubes.[57,58] With a shorter alkyl chain, the homologues, **13a**L and **13a**D, can form a hydrogel without the assistance of organic solvents. Left- and right-handed helical nanotubes were obtained from **13a**L and **13a**D, respectively. Similar results can also be observed from the acetonitrile gel of two dendron rod coils (DRC) molecules with opposite chirality, **13c*R*** and **13c*S***, synthesized by Stupp *et al.* These molecules self-assembled into beautiful mirror image helical nanostructures.[59] Although almost the same results were obtained from enantiomeric self-assembly (**13a** and **13c**), totally different nanostructures were obtained from the corresponding racemates. When equal moles of **13a**L and **13a**D were mixed, a white suspension rather than a hydrogel was formed with the appearance of smooth giant micro belts. On the contrary, the racemic mixture of **13c*R*** and **13c*S*** showed the same gelation properties as individual enantiomers and helical nanostructures rather than flat ribbons were generated.

The distinct results observed from racemic self-assembly can be ascribed to the different interaction between enantiomers. Specifically, heterochiral recognition usually induces the formation of flat or amorphous nanostructures, while homochiral recognition leads to the formation of self-sorted nanostructures. In the case of heterochiral interaction driving self-assembly, interesting results could frequently be obtained by varying the enantiomeric excess (ee) value of the enantiomer mixture and the excess of one enantiomer might have significant impact on the supramolecular chirality as well as the morphology.

Oda *et al.* developed a simple method to tune the geometrical parameters of chiral nanostructures (Fig. 14).[60] They found that the co-assembly of cationic gemini amphiphiles with chiral counter ions in chloroform led to the formation of stable twist ribbons. The chirality of such a kind of system comes from the counterion rather than from the amphiphile itself, so the parameter of the twist can be tuned by the introduction of chiral counterions with various ee values. They found that when racemic tartrate was used, only flat ribbons were obtained, equivalent to a twist with infinite pitch. The increase of ee value caused an obvious decrease of the twist pitch, along with the width. In this way, they firstly reported work about tuning bilayer twist nanostructures. Their work demonstrated that the properties of macroscopic chiral nanostructures could be controlled by variation of molecular chirality in an easy way.

In another recent report by our group,[61] Zhu *et al.* found that the mixing of enantiomers with different molar ratios could induce the emergence of different kinds of chiral nanostructures, as shown in Fig. 15. Both of the enantiomeric glutamic acid derivatives, **15**L and **15**D, self-assembled into ultralong tubular nanostructures through gel formation in ethanol, while only flat sheet-like structures were obtained from their racemate under the same conditions. Compared to the nanotubes formed by enantiomers, enhancement of hydrogen binding and elongation of *d*-spacing in the sheet-like structures were clearly revealed by IR and XRD measurements, suggesting the choice of self-recognition in racemic self-assembly. By varying the molar ratio of the two enantiomers, twist ribbons

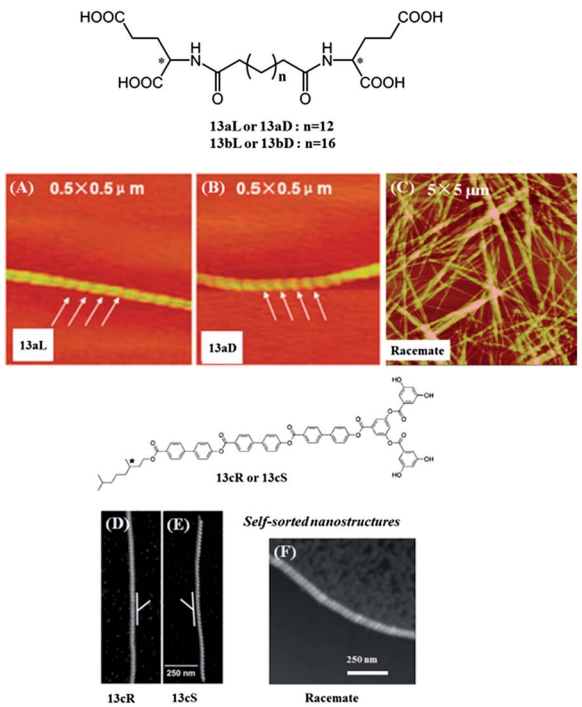

Fig. 13 Molecular structures of the glutamic acid derivatives, **13a**L, **13a**D, **13b**L and **13b**D and the dendron rodcoils **13c*R*** and **13c*S***. L, D, *R* and *S* represent the chirality of chiral groups in these molecules. (A–C) AFM images of the nanostructures formed by **13a**L, **13a**D and their racemate. (D–F) AFM images of the nanostructures formed by **13c*R***, **13c*S*** and their racemate. Adapted from ref. 57–59. Reprinted with permission from ref. 59. Copyright (2005) American Chemical Society.

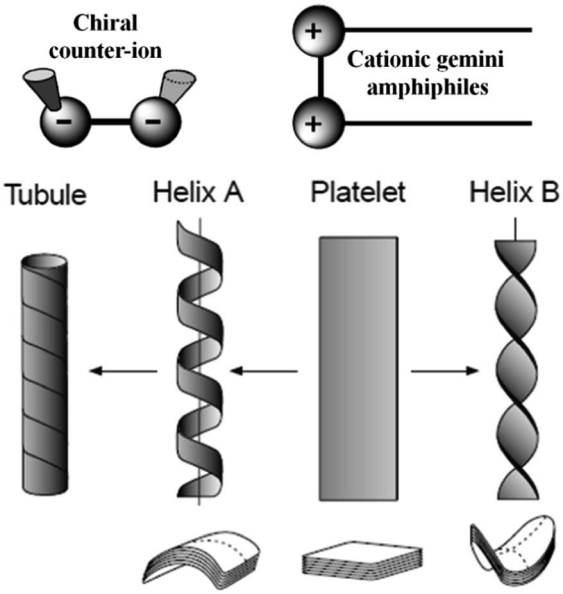

Fig. 14 Cartoon representation of the chiral counterion, cationic gemini amphiphiles and different types of nanostructures being formed. Reprinted with permission from ref. 60. Copyright (1999) Nature Publishing Group.

Published on 25 April 2014. Downloaded by Michigan State University on 24/01/2016 09:49:48.

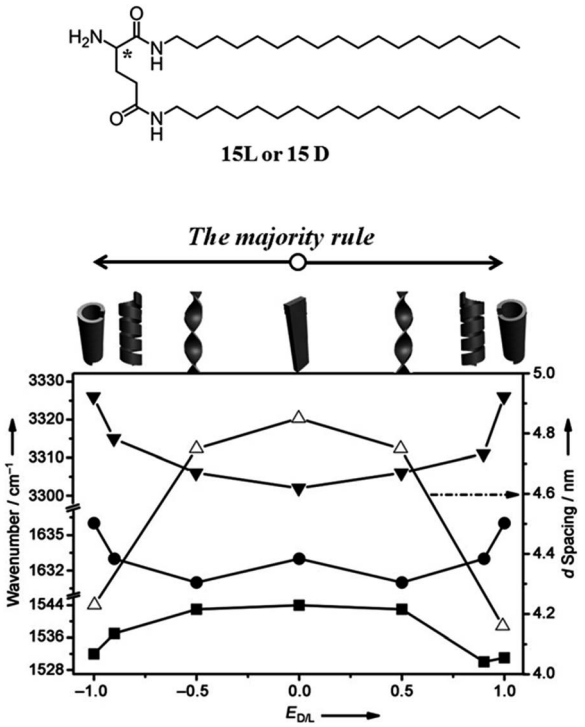

Fig. 15 Molecular structures of glutamic acid derivatives, **15**L and **15**D. L and D represent the chirality of glutamic acid. The bottom shows a cartoon representation and the plot of the vibration bands of N–H, amide I, amide II and the *d* spacing of the nanostructures in the mixed gels against the enantiomeric excess value. Reprinted with permission from ref. 61. Copyright (2010) John Wiley and Sons.

and rolled-up nanotubes were generated. The handedness of these chiral nanostructures was determined by the excess enantiomer. The excess of L-type enantiomer led to the formation of right-handed nanostructures, and whereas mirror-image nanostructures were obtained when excess D-type enantiomer was used, following the 'majority rule'. Thus, upon mixing the enantiomers in different ratios, we realized controlled fabrication of various chiral nanostructures.

In all the above cases, all the obtained chiral structures follow the 'majority rule'. However, a contrary way, in which the mixtures of achiral analogue and chiral molecule follow the 'sergeants and soldiers' principle, has been discovered. In this case, the handedness of the nanostructures can hardly be determined. Normally equal numbers of left- and right-handed ones are exhibited at the same time. As a consequence, the whole system should be CD silent. The introduction of a trace chiral dopant can induce dramatic changes to both the chirality and helicity of the racemic chiral nanostructures, following the 'sergeants and soldiers' principle. Hong and co-workers found that a simple achiral molecule,[62] **16**, can self-assemble into beautiful twist ribbons, showing left- or right-handedness simultaneously, while only amorphous nanostructures were obtained from corresponding analogical alanine derivatives, **16**L and **16**D (Fig. 16). Moreover, doping with no more than 1% chiral molecules was enough to induce the emergence of exclusively left- or right-handed twists, along with emergence of

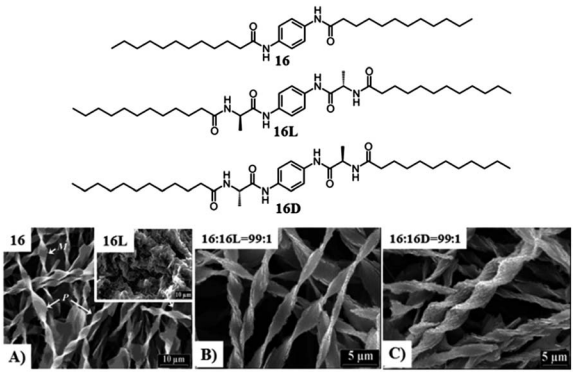

Fig. 16 Molecular structures of **16**, **16**L and **16**D. (A) SEM images of the xerogel of (A) **16**, (B) **16** : **16**L = 99 : 1, (C) **16** : **16**D = 99 : 1. Inset: SEM image of the xerogel of **16**L. L and D represent the chirality of alanine group. Reprinted with permission from ref. 62. Copyright (2008) John Wiley and Sons.

intense CD signals. The handedness of the twists was completely determined by the chirality of the dopant.

In some other cases, neither chiral molecules nor the achiral analogue form chiral nanostructures, while the co-assembly of chiral and achiral molecules leads to the formation of chiral nanostructures. Ajayaghosh *et al.* investigated the self-assembly of chiral and achiral oligo(*p*-phenyleneethynylene)s,[63] as well as their co-assembly (Fig. 17). The achiral molecule, **17a**, could form an organogel in nonpolar hydrocarbon solvents with the emergence of vesicles, and is CD silent. However, the chiral analogue **17b** failed to form aggregates under the same conditions. Dramatic changes appeared when various molar ratios of **17b** were used as dopant. With the increase of **17b**, helical nanotubes appeared with the gradually disappearance of vesicles, along with the increase in CD intensity. In this case, the doping of the chiral molecule not only determines the helicity,

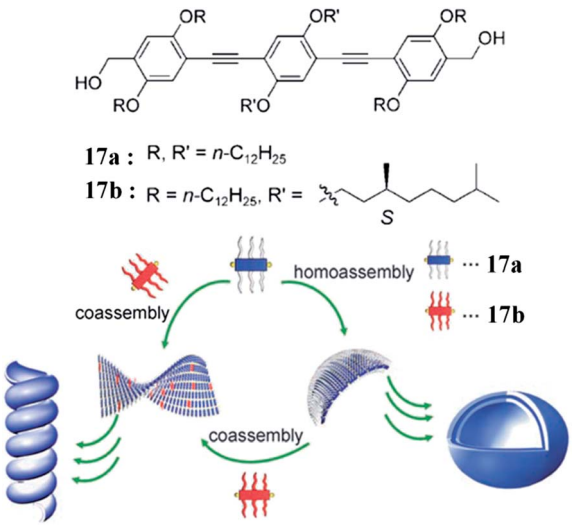

Fig. 17 Oligo(*p*-phenyleneethynylene) based molecules **17a** and **17b** and schematic illustration of their self-assembly in decane. Reprinted with permission from ref. 63. Copyright (2006) John Wiley and Sons.

This journal is © The Royal Society of Chemistry 2014

Published on 25 April 2014. Downloaded by Michigan State University on 24/01/2016 09:49:48.

but also leads to the formation of chiral nanostructures. Their results showed another kind of example of the 'sergeants and soldiers' principle.

Ajayaghosh and co-workers also showed us an abnormal example of the 'sergeants and soldiers' rule in a gel system.[32] They investigated the self-assembly of oligo(*p*-phenylenevinylene) (OPV) derivatives, **18a** and **18b**, in dodecane. **18b** with chiral side chains was able to self-assemble into left-handed helical nanostructures, while entangled tapes with no helical sense were obtained from achiral **18a**. These results seem reasonable. Mixing **18b** and **18a** together in dodecane (1.67 mol% of **18b**) at a total concentration of 7.5×10^{-4} M resulted in a split CD signal with positive and negative Cotton effects. The intensity of the signal reached its highest as the composition of **18b** increased up to 22 mol% (Fig. 18). Surprisingly, right-handed along with a few left-handed helical tapes appeared and the ratios of left-handed helices increased as the molar ratio of **18b** increased. Unlike the work on the 'sergeants and soldiers' principle reported previously, the soldiers, **18a**, seem to mistake orders from the chiral instructions of the sergeants, **18b**, and induce the formation of helical nanostructures with opposite handedness. Moreover, a helical junction, which is the joint between left-handed and right-handed helices, was also firstly observed in their experiments.

3.2 Molecular structure tuned chiral nanostructures

Apart from molecular chirality, another factor that affects the formation of chiral nanostructures is the molecular structure. Totally different nanostructures can be obtained from molecules with the same chiral centre and similar structures. As mentioned before, the chirality transfer from a chiral centre to a chromophore is determined by intermolecular or intramolecular interactions, so is the self-assembled nanostructures, as shown in Fig. 19. The three isomeric pyridine-containing L-glutamic lipids, **2a–c**, formed organogels in DMSO and self-assembled into different nanostructures of nanofibers, nanotwists and nanotubes depending on the substituent position in the pyridine ring.[23] Clearly, the three isomers have the same chiral centre in the glutamate segment, but totally different nanostructures were obtained. In the case of **2a**, the intermolecular H-bonds weakened the packing between the molecules and thus 2PLG only assembled into nanofibers, while the efficient intermolecular hydrogen bonds and chirality transfer in the molecular packing of **2b** and **2c** resulted in the formation of twist and nanotubes.

The Ajayaghosh group recently reported interesting work about different chiral nanostructures derived from similar building blocks,[64] as shown in Fig. 20. **20a** and **20b** are the mono- and disubstituted cholesterol-appended OPVs, respectively. Both of them could gel decane but with different critical gel concentrations. The differences in molecular packing were revealed by optical, chiroptical and morphology measurements. The maximum absorption of **20a** in decane at 20 °C was red shifted, while the corresponding absorption of **20b** was blue shifted. The CD spectra of **20a** and **20b** were almost mirror-images, though the observed microstructures showed the same right-handed (*P*) helical fibers. The model proposed by the authors suggests that a well-organized twisted helical arrangement of the chromophores is adopted by symmetrical molecule **20b**, while a tilted packing of the chromophores is favored by the hydrogen-bonded pair of the monocholesterol derivative **20a**. The extension of twist packing leads to the formation of twist nanostructures, while the tilted packing results in the formation of rolled-up helices. Their research clearly demonstrated how the molecular structures affect the molecular packing, which contributes further to the emergence of different nanostructures. This work provided a novel approach for the controlled fabrication of chiral nanostructures though molecular design.

3.3 Stimulus-responsive chiral nanostructures

In general, the helicity of gelation-induced chiral assemblies is the supramolecular chirality of molecular aggregates transferred from molecular chirality by non-covalent interactions. Some external stimuli, including light irradiation, heating and dopant, might have significant impact on the molecular

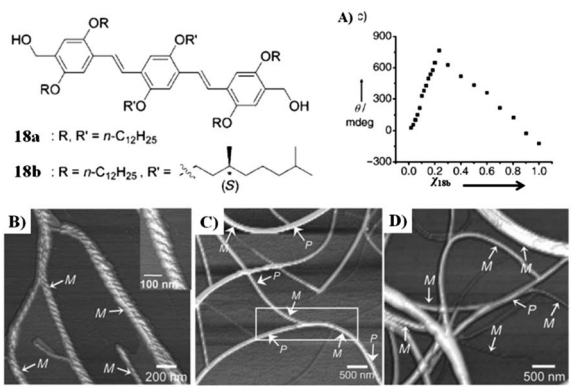

Fig. 18 Structures of the achiral and chiral molecules, **18a** and **18b**, under investigation. (A) Changes in the CD intensity at 420 nm during the coassembly of **18a** and **18b** in dodecane at different compositions. χ_{18b}: the molar ratio of **18b**. AFM height images of: (B) **18b** homoassembly, (C) coassembly of **18a** with 9 mol% of **18b**, and (D) coassembly of 18a with 60 mol% of **18b**. Reprinted with permission from ref. 32. Copyright (2005) John Wiley and Sons.

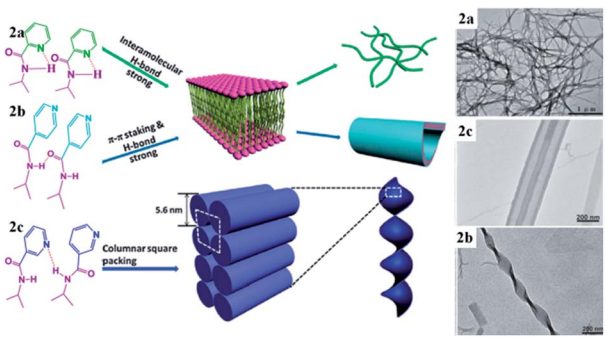

Fig. 19 Schematic illustration of the different self-assembly manners of **2a–c**. Adapted from ref. 23.

Published on 25 April 2014. Downloaded by Michigan State University on 24/01/2016 09:49:48.

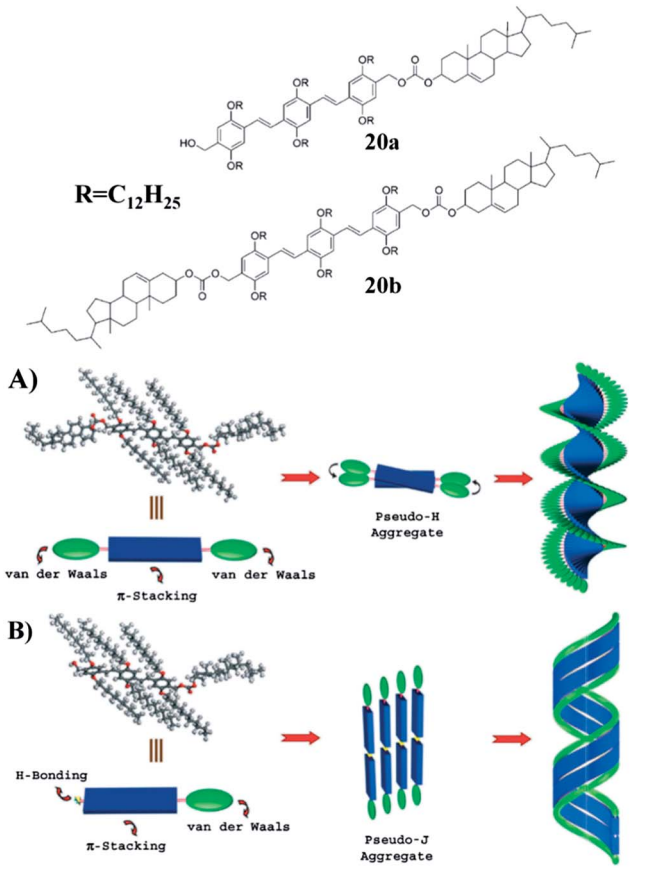

Fig. 20 The mono- and disubstituted cholesterol-appended OPVs, **20a** and **20b**. Proposed model for the self-assembly mechanism of **20a** (A) and **20b** (B) in decane. Reprinted with permission from ref. 64. Copyright (2006) John Wiley and Sons.

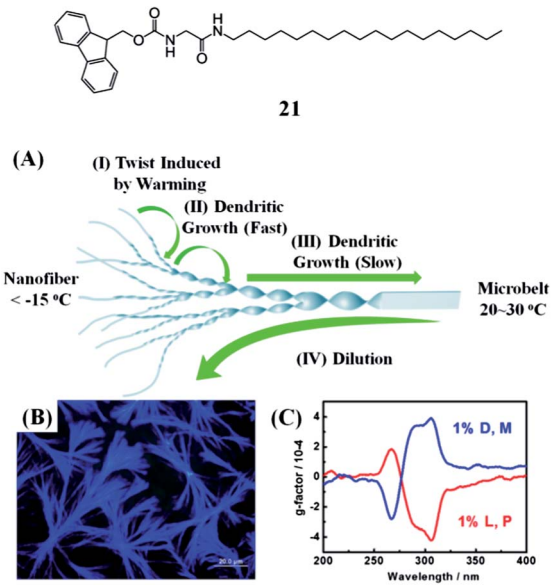

Fig. 21 Glycine derivative **21**. (A) Schematic illustration of the hierarchical dendrite twist structure formed by **21**. (B) Fluorescence microscopy images of the dendritic twists formed during step I and step II. (C) CD spectra of the dendritic twists doped with 1% molar ratios of chiral analogues. The analogous alanine derivatives are abbreviated to L and D, respectively. Reprinted with permission from ref. 65. Copyright (2012) American Chemical Society.

packing being formed, which further leads to the morphological transformation of chiral nanostructures. Various stimuli-responsive chiral nanostructures based on gel systems have been reported in an important approach for understanding the chiral self-assembly mechanism.

We found that an achiral glycine derivative, **21**, could gel ethyl acetate either at low temperature (<−15 °C) or room temperature with distinct gelation properties (Fig. 21).[65] The critical gelation concentrations has a six-fold difference and totally different nanostructures were formed. Nanofibers with width of about 50 nm were formed at low temperature, while giant microbelts with sizes of a few micrometers in width and hundreds of micrometers in length were obtained at room temperature. However, no helical sense was observed in either case. Dramatic changes were observed when the gel formed at low temperature was transferred to room temperature. Twisting of the nanofibers immediately occurred and they developed into dendritic twist nanostructures. Although both left-handed and right-handed twists showed up simultaneously, all the twists at the same dendritic structure exhibited the same handedness. When trace analogical alanine derivative was added, homochiral left- or right-handed dendritic twists could be obtained, following the 'sergeants and soldiers' principle. As time went by, the dendritic growth of the twist finally led to the formation of giant microbelts, achieving the temperature induced morphology transformation. More importantly, a reverse process to transform the microbelts into dendritic twists could be realized by simply diluting the gel formed at room temperature with ethyl acetate. A simple achiral molecule was utilized here to realize temperature, concentration and chirality responsive self-assembly. This research sheds new light on the hierarchical transformation of chiral structures from achiral molecules *via* controlled self-assembly.

We found the first example that the chiral twist can be easily tuned by using a broad range of metal ions (Fig. 22).[66] Terephthalic acid substituted amphiphilic L-glutamide, **22a–c**, could form a gel in DMSO, which can self-assemble into uniform helical twists in the presence of various metal ions, such as Fe^{3+}, Co^{2+}, Ni^{2+}, Cu^{2+}, Cd^{2+}, Mn^{2+}, Mg^{2+}, Li^{+}, Na^{+}, Ca^{2+}, Ag^{+}, Eu^{3+} and Tb^{3+}. When rare earth metal ions such as Eu^{3+} or Tb^{3+} were introduced, emissive nanotwists could be obtained. Moreover, the formation of the chiral twist is essentially reversible, the chiral twist disappeared upon adding 1,10-phenanthroline, and chiral twist would appear again when metal ions were added. The gelator of terephthalic acid substituted amphiphilic L-glutamide is suggested to form a bilayer structure at first. When the hydrophilic part was tuned by the metal ions, the multilayer structure transformed to chiral twists. The results present an easy way to obtain chiral twists by introduction of metal ions.

Hamachi *et al.* synthesized a bolaamphiphile by the Diels–Alder reaction.[67] They used a hydrogelator bearing a dienophile and a water-soluble diene to produce the molecule **23** (Fig. 23).

This journal is © The Royal Society of Chemistry 2014

Published on 25 April 2014. Downloaded by Michigan State University on 24/01/2016 09:49:48.

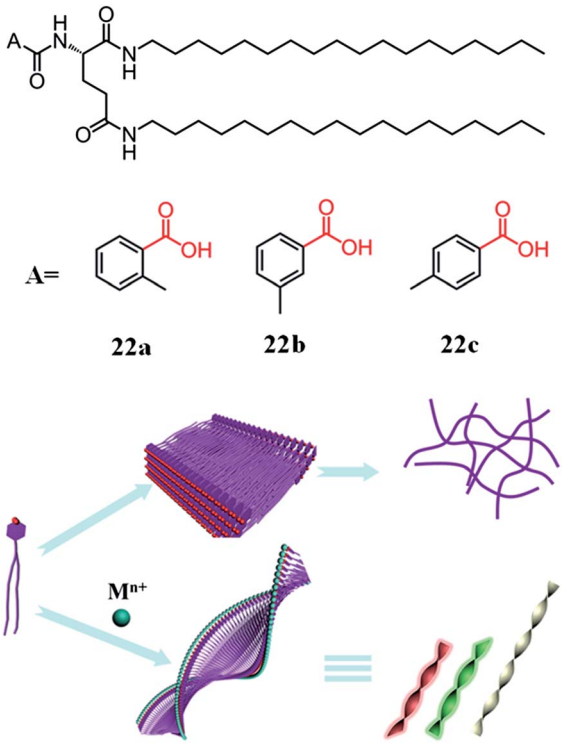

Fig. 22 Terephthalic acid substituted amphiphilic L-glutamide **22a**, **22b** and **22c** and scheme illustration of their self-assembly in DMSO with and without metal ions. Adapted from ref. 66.

This molecule self-assembled into short 2D nanosheets in water. The retro-Diels–Alder reaction was triggered upon heating, leading to the cleavage of the maleimide–furan pair and the formation of a hydrogelator. Accordingly, a supramolecular hydrogel was formed with the appearance of remarkable morphological transformation. Well-defined 1D left-handed helical ribbons were formed with the same character of those obtained from the individual hydrogelator. Their research provides a rational molecular design toward heat-induced supramolecular hydrogel formation, as well as an excellent example of heat-stimulus responsive supramolecular nanostructures.

A pyridylpyrazole linked L-glutamide organogelator (**24**) can self-assemble into diverse nanostructures over a wide range from nanofiber to nanotube and microtube depending on the solvent polarity (Fig. 24).[68] The nanofiber, nanotwist, nanotube and microtube structures of **24** were obtained in toluene, chloroform, DMF and DMSO, respectively. Such morphological changes can even occur for the xerogels upon exposure to the solvent vapours. It is suggested the interaction between the pyridylpyrazole headgroup and the solvents may subtly change the stacking of the molecules and thus their self-assembled nanostructures. Thus, by choosing appropriate solvents, a transition of morphology from nanofibers to chiral twists to nanotubes, and to microtubes can be achieved.

3.4 Replica of chiral nanostructure to inorganic materials

Chiral information can be translated into nano-/micro-scale assemblies as a consequence of controlled non-covalent interactions. There has been considerable interest in whether the chiral information encoded within the gel-phase assembly can subsequently be transcribed into other types of material.

Generally, a nanostructured gel can be used as a template for subsequent materials synthesis. The final product of the transcription process can be an organic–inorganic hybrid or purely

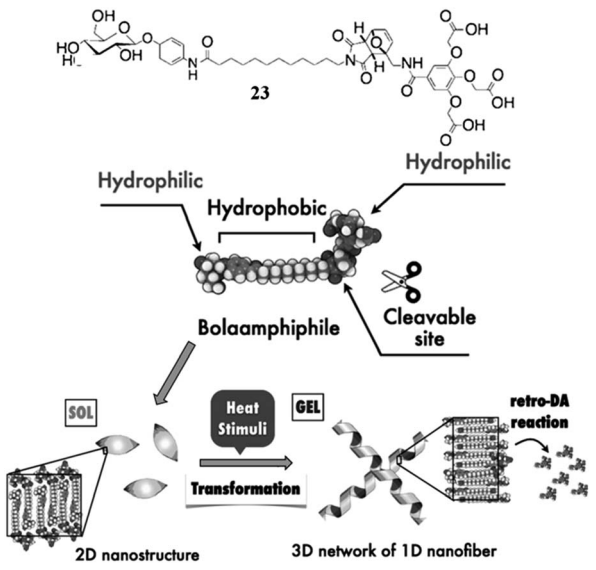

Fig. 23 Molecular structure of **23** and schematic representation of the heat-induced morphological transformation. Reprinted with permission from ref. 67. Copyright (2012) John Wiley and Sons.

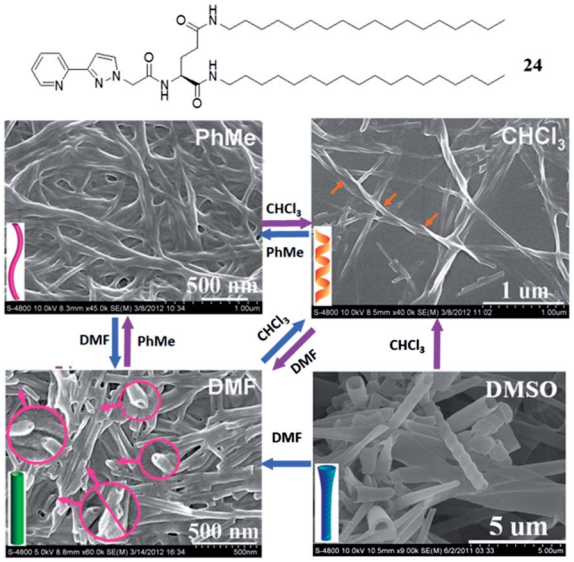

Fig. 24 The morphological changes of xerogel **24** responsive to solvent vapour: toluene vapour; $CHCl_3$ vapour and DMF vapour. While the morphologies can be switched between nanofibers, twists and nanotubes, they cannot be tuned to microtubes. However, the microtubes can be switched into nanotubes and nanotwists. Reprinted with permission from ref. 68. Copyright (2013) John Wiley and Sons.

Published on 25 April 2014. Downloaded by Michigan State University on 24/01/2016 09:49:48.

inorganic depending on whether or not the organic template has been removed. This approach has developed very rapidly in the last few years. Some review articles have summarized the recent work on chiral transcription from supramolecular chirality to inorganic nanomaterials. The literature is already far too rich to make an exhaustive presentation in the context of this chapter, and we have limited the scope of this section to a few examples. For more details, we refer the reader to several review articles.[54,69] Stupp and co-workers have demonstrated the transcription of chiral information from chiral gelator to inorganic nanostructures.[70] As shown in Fig. 25, by using a chiral self-assembling 'dendron–rod–coil' gelator, helical CdSe nanostructures can be fabricated by the template method. Electron microscopy revealed the presence of helical CdSe fibres after polymerization of the starting materials in the presence of a chiral gelator.

The Kobayashi group also reported several pioneering works on chiral transcription of helical fibers of gels onto silica and metal oxides.[71] Bola amphiphile molecule **26** (as the perchlorate salt) gelled ethanol with the formation of helical aggregates and the sol–gel polymerization of metal alkoxides of titanium, tantalum and vanadium was carried out on these chiral fibers. Basic hydrolysis of a mixture containing the metal alkoxides and the gelator in ethanol led to helical metal oxide structures, implying the successful transcription of chiral sense to the metal oxide. Typical SEM pictures obtained for the tantalum oxide fibers with right-handed and left-handed helicity, prepared using the *R*,*R* and *S*,*S*-enantiomers as the gelators, respectively, is shown in Fig. 26.

The helical nanotubes generated by **13a**L and **13a**D were further used as templates for the preparation of silica nanotubes (Fig. 27). After the removal of helical templates, free amino groups were embedded along the inner wall of silica nanotubes.[58] Interestingly, the supramolecular chirality of helical nanotubes was transferred to the inner wall, as confirmed by absorbing an achiral porphyrin derivative with sulfonic acid groups (TPPS). Intense CD signals were observed and mirror-imaged CD spectra were obtained from silica nanotubes prepared from helical nanotubes with opposite handedness, suggesting the transcription of supramolecular chirality. We further covalently attached azobenzene moieties to the inner wall and also induced chirality was observed. The CD signals also showed reversible changes upon alterative UV/vis irradiation, thus a novel chiroptical switch was generated.

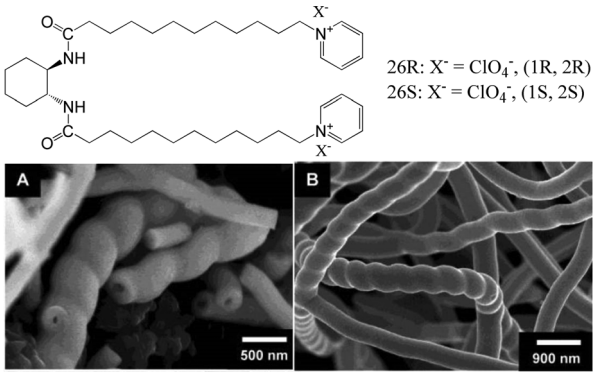

Fig. 26 Gelator 26 and SEM images of tantalum oxide fibers obtained from (A) 26*R* and (B) 26*S*. Reprinted with permission from ref. 71. Copyright (2002) American Chemical Society.

Another topic on chiral inorganic nanostructures is the chiral metals or metal clusters that show surface-plasmon circular dichroism (SP-CD). Although intensive chiral materials have been fabricated from organic and inorganic chiral species, chiral metals or metal clusters are very limited. Recently, there has been a surge of interest in the chirality of metal surfaces and metallic nanoparticles. Guerrero-Martinez, Liz-Marzan and co-workers have summarized the recent work on SP-CD.[72] The chiroptical activity may in principle be generated through two distinct origins: nanoparticles with individual chirality and collective interactions between 3D ordered nanocrystals. Generally, silver and gold are two famous noble metals in chiral nanoparticle research because of their excitation of localized

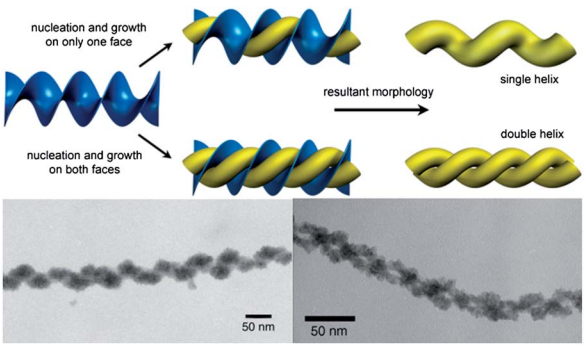

Fig. 25 Schematic representation of a possible templating mechanism in which a coiled CdS helix or double helix is produced from a twisted helical template through growth along the face of the template and TEM micrographs of the CdS helix and double helix. Reprinted with permission from ref. 70. Copyright (2002) John Wiley and Sons.

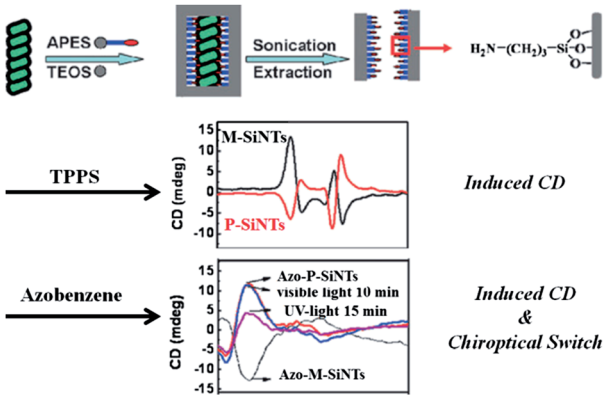

Fig. 27 Schematic illustration of the template preparation of silica nanotubes with chiral inner walls and its application for induced CD and chiroptical switch. The helical nanotube templates were obtained from hydrogels of **13a**L and **13a**D. M-SiNTs and P-SiNTs represent the silica nanotubes obtained from L- or D-glutamic acid based bolaamphiphiles, respectively. TPPS is the abbreviation for tetraphenylporphine tetrasulfonic acid. Adapted from ref. 58.

This journal is © The Royal Society of Chemistry 2014

Published on 25 April 2014. Downloaded by Michigan State University on 24/01/2016 09:49:48.

surface plasmon resonances. As mentioned above, most of the chiral nanoparticles were obtained by reducing a hybrid system composed of chiral inducers (cysteine and its derivatives) and metal starting materials (Ag^+, Au^{3+}). The reaction phase was the fluid phase. However, very few works have involved preparing optically active metal nanoparticles in nanocomposite gel systems.

Our group has reported one intriguing work on chiral silver nanoparticle fabrication through the *in situ* reduction of an organogel formed by a newly designed silver(I)-coordinated organogelator,[73] as shown as Fig. 28. Ag-coordinated lipid gelator **28b** could form a stable organogel in ethanol. After reduction by hydroquinone, chiral silver nanoparticles formed, which could be confirmed by CD measurements. TEM images demonstrated that the chiral silver nanoparticles were wrapped into the gel networks (Fig. 28A). It should be further noted that the use of a silver salt in the formation of chiral silver NPs is very important. No chiral signal could be detected if the gel was simply doped with the preformed silver nanoparticles. Moreover, the formation of the organogel process played an important role in the formation of the chiral nanoparticles. Thus, this is the first example of gelation-induced supramolecular chiral nanoparticles.

4. Application of gelation-induced supramolecular chirality

One of the reasons why supramolecular gels attract so much attention is their very high potential for applications. The last section of this review addresses applications that specifically make use of gelation-induced supramolecular chirality, such as those based on chiroptical switches, chiral recognition and asymmetric catalysis.

4.1 Chiroptical responsiveness

As we stated above, gelation-induced supramolecular chirality in chiral gel systems is the chirality of assembled aggregates transferred from molecular chirality by non-covalent interactions such as H-bonds, interchain interactions, π–π stacking and so forth. It is strongly related to the assembly model of gelator molecules. Thus, it is reasonable that the supramolecular chirality of gels is sensitive to environmental stimuli. Stimuli-responsiveness is the highlight of LMWGs.[74] Apart from thermal responsiveness, various physical gels also respond to other stimuli including light irradiation and redox, which can trigger the gel–sol transitions. By introducing chiral segments into the molecular design, various chiral LMWGs with external stimuli responsiveness have been explored.

Generally, the CD signal intensity of chiral gels relates to the gelation state. It will strengthen while gelator molecules are assembling and weaken as gelator molecules disassemble. Nearly all the chromophore-bearing chiral gels show a temperature dependent CD signal switch, accompanying a gel–sol transition. The CD signal disappears when the sol phase exists upon increasing temperature and reappears when the gels form upon cooling, indicating that the supramolecular chirality in gels shows thermal responsiveness.

There are two main strategies to achieve chiroptical switching based on gelation-induced supramolecular chirality: (i) a chiroptical switch composed of an intrinsically chiral gelator; (ii) a chiroptical switch constructed by a chiral/achiral hybrid gelator system. A chiroptical switch based on a totally achiral gelator is a higher pursuit in this kind of distinct smart material design. A chiroptical switch constructed by a chiral gelator is the most commonly reported in supramolecular gel field. Extensive reports have described thousands of chiroptical switches based on chiral gelators. Diverse thermo-, photoirradiation-, ultrasound- and electrochemistry-regulated supramolecular chirality reversible changes can be proposed into smart chiroptical switches.

Photo-regulated supramolecular chirality in chiral gels is a big issue in the supramolecular self-assembly gels field. Feringa's group,[75] Shinkai's group[76] and Weiss's group[77] have reported some original works with respect to this subject. A common feature is introducing a photoactive group to a chiral gelator molecule, which will construct a photoactive chiral gelator.[78–82] Diarylethene and azobenzene are two famous photoisomerization groups that have been widely studied in photoregulated supramolecular gels. In particular, the azobenzene group has been utilized in hundreds of works because of its easy synthesis and excellent photoisomerization character in supramolecular assembly systems.

Our group has reported a glutamate based lipid gelator bearing an azobenzene segment, which showed excellent photoregulated gel–sol transition (Fig. 29).[28] Gelation-induced supramolecular chirality can be tuned by UV/visible light. However, the photo-triggered azobenzene supramolecular chirality has a strong relationship with gelation solvent. In this case, the chiral switch only arises in nonpolar solvents due to azobenzene segment isomerization in nonpolar solvents. In polar solvents, strong interchromophore interaction confined the activity of the azobenzene groups, which resulted in the silent photoisomerization (Fig. 30). Also, supramolecular chirality could not respond to photoirradiation.

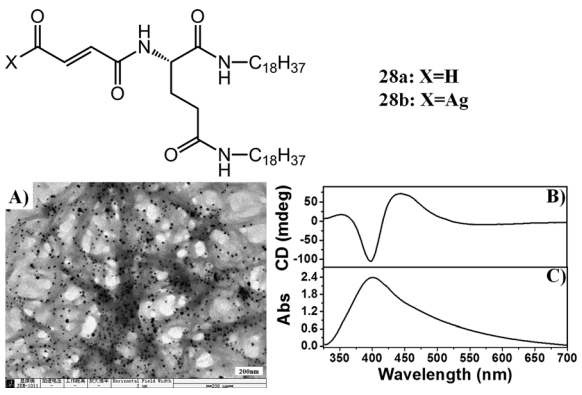

Fig. 28 Molecular structure of the gelator **28a** and silver(I)-coordinated gelator **28b**; (A) TEM image of the reduced xerogel; (B) CD and (C) UV-vis spectra of the prepared silver nanoparticles. Adapted from ref. 73.

Published on 25 April 2014. Downloaded by Michigan State University on 24/01/2016 09:49:48.

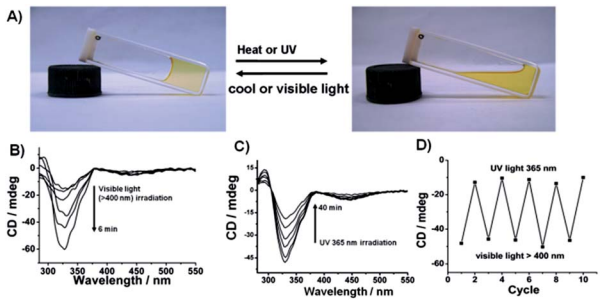

Fig. 29 (A–D) Photochemical reaction of azobenzene based chiral gelator **4** and the relative CD spectra. Reprinted with permission from ref. 28. Copyright (2011) American Chemical Society.

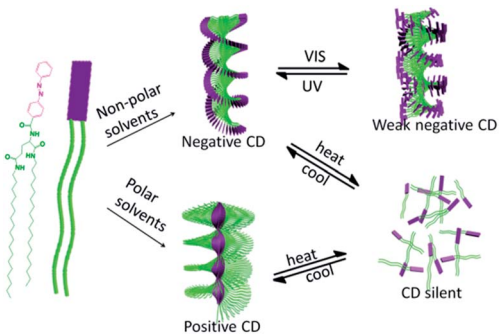

Fig. 30 Illustration of the multichannel supramolecular chiroptical switches composed of gelator **4**. The gelator molecules formed organogels showing negative CD in nonpolar solvents and positive CD in polar solvents. Both of the gels showed reversible changes in chirality upon heating and cooling cycles. The organogels formed in the nonpolar solvents could show additional photoresponse upon alternate UV/vis irradiation. Reprinted with permission from ref. 28. Copyright (2011) American Chemical Society.

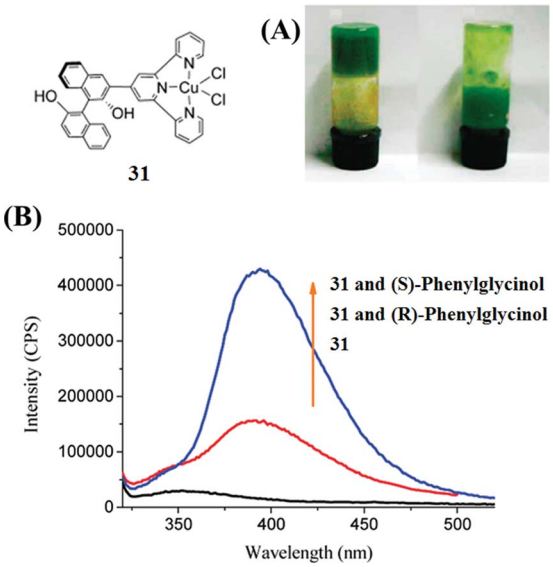

Fig. 31 Molecular structure of the gelator **31**. (A) Visual enantioselective responses of the gel of **31** toward (*R*)-phenylglycinol (left) and (*S*)-phenylglycinol (right). (B) Fluorescence spectra of **31** (5.0×10^{-7} M) in CH_2C_{l2}–*n*-hexane (2 : 3) in the presence of (*R*)- and (*S*)-phenylglycinol (5.0×10^{-4} M) (λ_{exc} = 289 nm, slits: 2 nm/5 nm). Reprinted with permission from ref. 83. Copyright (2010) American Chemical Society.

4.2 Chiral recognition

One important application of gelation-induced supramolecular chirality is chiral recognition, which also is at the heart of all natural processes.[6] Converting chiral interaction information into a readable output is scarce, especially in supramolecular gel systems. Generally, chiral recognition proposed by gelation-induced supramolecular chirality exhibits the following characteristics. (i) Chiral recognition in gel systems is different to other intermediates such as solution or solid phase. Both spectral measurement and the observation of the gel state can be used to monitor the recognition. (ii) Induced supramolecular chirality is expressed in the macroscopic chiral structure, which is reversible by environmental stimuli. Chiral recognition in supramolecular systems is the result of chiral interaction between gel aggregates and guest chiral molecules.

Yu, Pu and co-workers have reported a case of chiral sensing.[83] As shown in Fig. 31, by sonication for 1 min, chiral gelator **31** could form a stable gel by mixing with (*R*)-phenylglycinol (0.10 equiv.) in $CHCl_3$ (0.1 mL), while the gel collapsed after mixing with (*S*)-phenylglycinol (0.10 equiv.) in $CHCl_3$ (0.1 mL). This may be due to the amino alcohol displacing the Cu(II) ion from the ligand in **31**. Spectral measurement confirmed that the interaction of the gelator **31** with (*S*)-phenylglycinol was totally different from the gelator **31** with (*S*)-phenylglycinol. Additionally, the chiral Cu(II) complex also exhibited significant enantioselective fluorescent enhancement in the presence of a variety of amino alcohols (Fig. 31 B). The more favorable interaction of **31** with (*S*)-phenylglycinol observed in solution might be greatly amplified in the supramolecular assembly of the gel network, leading to the visually enantioselective response. This work shows the most convenient visual detection method for chiral recognition in supramolecular gel systems.

Tu *et al.*[84] established a visual chiral recognition system for (*R*)- and (*S*)-binap based on an enantiocontrolled breakdown of gels prepared from novel ALS-type pincer metallogelators **32a** and **32b** (Fig. 32). A ^{31}P NMR spectroscopy study of metallogel **32a**/$CDCl_3$ (1 wt%) in the presence of one equivalent (*R*)- or (*S*)-binap confirmed that the chirality of (*R*)-binap matched the chiral environment of the cholesterol fragment directly attached to the pincer heteroaromatic rings. Thus, the coordination to the Pt centre of biphosphine caused the blocking of π–π stacking and metal–metal bonds owing to the hindrance of the bulky binaphthalene skeleton and the PPh_2 group. Finally, the assembly of the metallogelator molecules is blocked, leading to the collapse of the gel. (*S*)-Binap, however, is unmatched to the chiral metallogelator and consequently has no major impact on the assembly process.

Recently, our group also addressed some interesting chiral recognition cases in supramolecular organogel systems.[85–89] Here, we select one example as an introduction.[88] Schiff base organogelator **33** could form organogels in DMSO due to the

 This journal is © The Royal Society of Chemistry 2014

Published on 25 April 2014. Downloaded by Michigan State University on 24/01/2016 09:49:48.

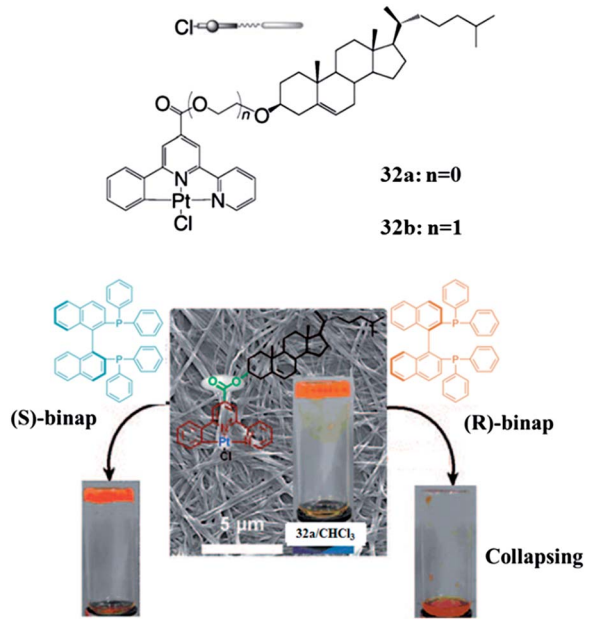

Fig. 32 The visual chiral recognition of (*R*)- and (*S*)-binap has been realized through an enantioselective breakdown of metallogels prepared from **32**. van der Waals interactions, π stacking, and metal–metal bonding are responsible for the aggregation and chiral recognition. Reprinted with permission from ref. 84. Copyright (2011) John Wiley and Sons.

synergistic effects of π–π interactions, H-bonding and hydrophobic interactions. Additionally, after mixing with Mg^{2+}, a stable chiral metallogel could be obtained, showing strong emission. More interestingly, the Mg^{2+}-mediated metallogel showed chiral recognition towards D- and L-tartaric acid, whilst the corresponding un-gelated solution did not. As shown in Fig. 33, the approach of D-tartaric acid toward the Mg^{2+} ions was stereochemically more favourable on the surface of the nanofiber and hence caused a more significant quenching of the fluorescence than L-tartaric acid.

A highly ordered chiral assembly of achiral porphyrin on a chiral molecular gel also realized enantioselective recognition of amino acid methyl esters (Fig. 34).[90] The fluorescence quenching of porphyrin in molecular gels was more effective in the presence of the L-enantiomer than in that of the D-enantiomer, while in chloroform, in which the porphyrin existed in the monomer state, there was no significant difference in quenching rates between the L and D enantiomer. These recognition results were brought about by chiral ordered stacking of the binding sites but not by molecular chirality.

4.3 Asymmetric catalysis

Supramolecular gels can be considered as self-supported catalytic heterogeneous phases, and in contrast to classical solid-supported heterogeneous catalysts, the use of LMWGs and non-covalent interactions to build up the catalytic phase allow for simple synthetic procedures and easy access to libraries of potential catalysts. Furthermore, the reversible nature of these systems affords easy recovery of the catalyst not only by filtration at the end of reaction but by pH or temperature change. Recently, supramolecular gels as media for organic reactions have gained more and more interest due to their distinctive characteristics: (i) coexistence of solid-like networks and flowing phase; (ii) the solid network structures are easy to regulate and the assembled supramolecular structures are diverse; (iii) abundant liquid/solid boundary; (iv) reversible gel–sol transition, easy recycling; (v) activity and selectivity in gel phase is quite insensitive to temperature and concentration changes. Miravet and co-workers have reviewed some recent work concerning supramolecular gels as active media for organic catalysis.[91] Here, we would like to focus on chiral catalysis and introduce the application of gelation-induced supramolecular chirality in asymmetric catalysis. One outstanding pioneering work was reported by Miravet and co-workers.[92] As shown in Fig. 35, L-proline amphiphilic derivative **35** can form a hydrogel at a concentration of 2 mM. This kind of hydrogel can be used as a heterogeneous catalytic system for the direct aldol reaction between cyclohexanone and 4-nitrobenzaldehyde. Interestingly, at low temperature (5 °C), both the reaction yield and selectivity were incredible high (yield: 98%; ee: 88%). It should be

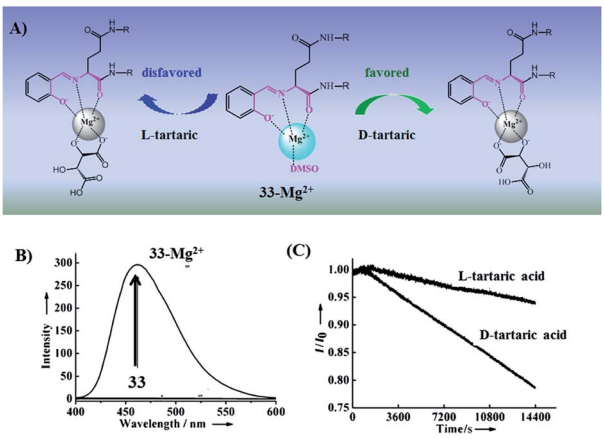

Fig. 33 (A) Schematic illustration of the chiral recognition of the Mg^{2+} coordinated Schiff base gelator **33**–Mg^{2+} towards tartaric acid. (B) Fluorescence spectra of the Schiff base gelator before and after forming a complex with Mg^{2+}. (C) Fluorescence quenching of tartaric acid by the Mg^{2+}-mediated gel *versus* time. Reprinted with permission from ref. 88. Copyright (2012) John Wiley and Sons.

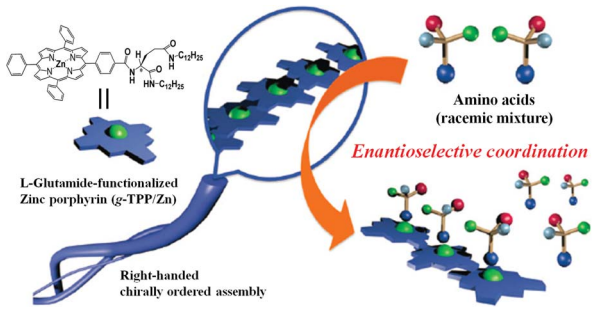

Fig. 34 Schematic image of the enantioselective recognition through chiral ordered porphyrin assembly. Adapted from ref. 90.

Published on 25 April 2014. Downloaded by Michigan State University on 24/01/2016 09:49:48.

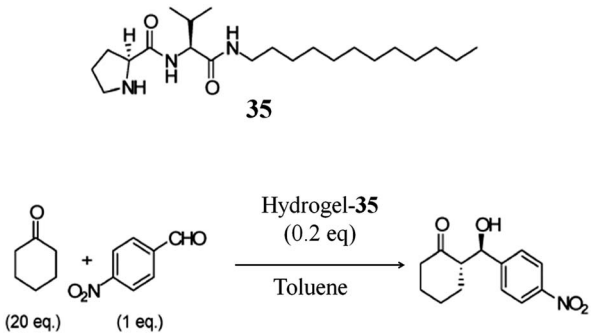

Fig. 35 Schematic representation of the direct aldol reaction catalysed by hydrogelator **35**. Adapted from ref. 92.

emphasized that the assembled fibrillar structures are the main catalytic agent. The observed catalytic activity could arise from the heterogeneous gel phase. Gelator molecular chirality was transferred to the assembled fibrillar structures after gelation, and the induced chirality can control the reaction selectivity. They have given a detailed study of the influence of molecular self-assembly into fibrillar nanostructures on the chiral catalysis as well as the molecular mechanism.[93]

Recently, we have shown an example of supramolecular gel supported chiral catalysis.[94] As shown in Fig. 36, bolaamphiphile gelator **13a** formed a hydrogel in water with a tubular structure. The addition of Cu^{2+} ions caused a transition from monolayer nanotube to multilayer nanotube. The formed Cu^{2+}-mediated nanotube can be used as an asymmetric catalyst for Diels–Alder cycloaddition between cyclopentadiene and aza-chalcone. In comparison with the other complexes formed by Cu^{2+}–glutamic acid derivatives, Cu^{2+}-mediated nanotube structures showed not only accelerated reaction rate, but also enhanced enantiomeric selectivity (ee: 51%). It was suggested

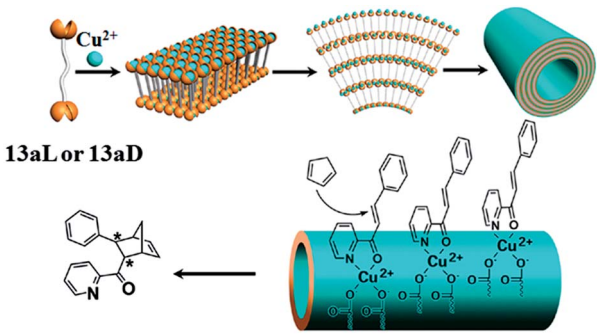

ligand	yield	endo/exo	ee[endo]
13 aL	89%	97:3	51
13 aD	87%	96:4	-51

Fig. 36 Illustration of the assembly mechanism of Cu^{2+}–**13a**L (**13a**D) tubular structure and its asymmetric catalysis for Diels–Alder reaction of aza-chalcone with cyclopentadiene. The results are listed in the table below. Reprinted with permission from ref. 94. Copyright (2011) American Chemical Society.

that through the Cu^{2+}-mediated nanotube formation, the substrate molecules could be anchored on the nanotube surfaces and produced a stereochemically favored alignment. When the adducts reacted with the substrate, both the enantiomeric selectivity and the reaction rate increased. Since the Cu^{2+}-mediated nanotubes can be fabricated easily and in large amounts, the work opens a new way to perform efficient chiral catalysis through supramolecular gels.

Another example is the enantioselectivity in a binary gel system reported by Shinkai and Fujita.[95] A binary gelator containing 2-anthracenecarboxylic acid (2Ac) non-covalently linked to 3,4,5-tris(*n*-dodecyloxy)-benzoylamide substituted D-alanine can act as an efficient gelator of a nonpolar solvent like cyclohexane. The photo-cyclodimerization of the 2Ac in the gel matrix favoured only h–h photodimers with a significant ee value 10% while no effective ee value could be obtained in other states: solution state or solid state. Thus, gelation-induced supramolecular chirality can control the stereochemical selectivity of photodimers. The gel structure, or in other words the orientation of 2Ac molecules in the gel matrix, is the key factor to the h–h photodimers' formation. This work can be considered as a new approach towards supramolecular gel supported chiral catalysis.

5. Conclusion and perspectives

In summary, this review has demonstrated examples of gelation-induced supramolecular chirality. As an important and fascinating research topic in LMWG systems, it plays a more and more important role in understanding self-assembly mechanisms and developing fascinating chiral materials. This review illustrated the types, formation mechanism and special characteristics of gelation-induced supramolecular chirality and introduced some typical applications in optical devices, catalysis and chiral recognition. We envisage that these general concepts could be widely applicable to push back the frontiers of supramolecular chemistry.

In comparison with gels from polymers, supramolecular gels are generally physical gels. The reversibility and the stimuli-responsiveness of the gel systems will endow the supramolecular chirality in gels with unique properties. More structural and functional chiral systems are expected to be developed.

Acknowledgements

This work was supported by the Basic Research Development Program (2011CB932301 and 2010CB833305), the National Natural Science Foundation of China (no. 91027042, 21021003, 21321063), and the Fund of the Chinese Academy of Sciences.

Notes and references

1 J. Cornelissen, A. E. Rowan, R. J. M. Nolte and N. Sommerdijk, *Chem. Rev.*, 2001, **101**, 4039–4070.
2 J. G. Rudick and V. Percec, *Acc. Chem. Res.*, 2008, **41**, 1641–1652.

 This journal is © The Royal Society of Chemistry 2014

Published on 25 April 2014. Downloaded by Michigan State University on 24/01/2016 09:49:48.

3 E. Yashima, K. Maeda and Y. Furusho, *Acc. Chem. Res.*, 2008, **41**, 1166–1180.
4 D. J. Hill, M. J. Mio, R. B. Prince, T. S. Hughes and J. S. Moore, *Chem. Rev.*, 2001, **101**, 3893–4011.
5 M. S. Spector, J. V. Selinger, J. M. Schnur, M. M. Green, R. J. M. Nolte and E. W. Meijer, in *Materials-Chirality*, John Wiley & Sons, Inc., New York, 2003, vol. 24, pp. 281–372.
6 G. A. Hembury, V. V. Borovkov and Y. Inoue, *Chem. Rev.*, 2008, **108**, 1–73.
7 O. Sato, *Acc. Chem. Res.*, 2003, **36**, 692–700.
8 B. L. Feringa and R. A. van Delden, *Angew. Chem., Int. Ed.*, 1999, **38**, 3419–3438.
9 B. L. Feringa, R. A. van Delden, N. Koumura and E. M. Geertsema, *Chem. Rev.*, 2000, **100**, 1789–1816.
10 L. Pu, *Chem. Rev.*, 2004, **104**, 1687–1716.
11 D. K. Smith, *Chem. Soc. Rev.*, 2009, **38**, 684–694.
12 R. M. Hazen and D. S. Sholl, *Nat. Mater.*, 2003, **2**, 367–374.
13 B. L. Feringa, *Acc. Chem. Res.*, 2001, **34**, 504–513.
14 A. R. Hirst and D. K. Smith, in *Low Molecular Mass Gelators: Design, Self-Assembly, Function*, ed. F. Fages, 2005, vol. 256, pp. 237–273.
15 A. Brizard, R. Oda and I. Huc, in *Low Molecular Mass Gelators: Design, Self-Assembly, Function*, ed. F. Fages, 2005, vol. 256, pp. 167–218.
16 O. Gronwald, E. Snip and S. Shinkai, *Curr. Opin. Colloid Interface Sci.*, 2002, **7**, 148–156.
17 L. A. Estroff and A. D. Hamilton, *Chem. Rev.*, 2004, **104**, 1201–1217.
18 P. Terech and R. G. Weiss, *Chem. Rev.*, 1997, **97**, 3133–3159.
19 A. Dawn, T. Shiraki, S. Haraguchi, S. Tamaru and S. Shinkai, *Chem. – Asian J.*, 2011, **6**, 266–282.
20 P. F. Duan and M. H. Liu, *Langmuir*, 2009, **25**, 8706–8713.
21 A. Fukuda, Y. Takanishi, T. Isozaki, K. Ishikawa and H. Takezoe, *J. Mater. Chem.*, 1994, **4**, 997–1016.
22 P. F. Duan and M. H. Liu, *Phys. Chem. Chem. Phys.*, 2010, **12**, 4383–4389.
23 P. F. Duan, X. F. Zhu and M. H. Liu, *Chem. Commun.*, 2011, **47**, 5569–5571.
24 J. X. Cu, Y. J. Zheng, Z. H. Shen and X. H. Wan, *Langmuir*, 2010, **26**, 15508–15515.
25 T. Y. Wang, Y. G. Li and M. H. Liu, *Soft Matter*, 2009, **5**, 1066–1073.
26 W. C. Still, A. Tempczyk, R. C. Hawley and T. Hendrickson, *J. Am. Chem. Soc.*, 1990, **112**, 6127–6129.
27 H. Z. Tang, P. D. Boyle and B. M. Novak, *J. Am. Chem. Soc.*, 2005, **127**, 2136–2142.
28 P. F. Duan, Y. G. Li, L. C. Li, J. G. Deng and M. H. Liu, *J. Phys. Chem. B*, 2011, **115**, 3322–3329.
29 L. Zhang, C. X. Liu, Q. X. Jin, X. F. Zhu and M. H. Liu, *Soft Matter*, 2013, **9**, 7966–7973.
30 P. C. Xue, R. Lu, X. C. Yang, L. Zhao, D. F. Xu, Y. Liu, H. Zhang, H. Nomoto, M. Takafuji and H. Ihara, *Chem. – Eur. J.*, 2009, **15**, 9824–9835.
31 J. X. Cui, A. H. Liu, Y. Guan, J. Zheng, Z. H. Shen and X. H. Wan, *Langmuir*, 2010, **26**, 3615–3622.
32 A. Ajayaghosh, R. Varghese, S. J. George and C. Vijayakumar, *Angew. Chem., Int. Ed.*, 2006, **45**, 1141–1144.
33 J. J. D. de Jong, T. D. Tiemersma-Wegman, J. H. van Esch and B. L. Feringa, *J. Am. Chem. Soc.*, 2005, **127**, 13804–13805.
34 A. R. Hirst, D. K. Smith, M. C. Feiters and H. P. M. Geurts, *Chem. – Eur. J.*, 2004, **10**, 5901–5910.
35 X. F. Zhu, P. F. Duan, L. Zhang and M. H. Liu, *Chem. – Eur. J.*, 2011, **17**, 3429–3437.
36 K. Lv, L. Qin, X. F. Wang, L. Zhang and M. H. Liu, *Phys. Chem. Chem. Phys.*, 2013, **15**, 20197–20202.
37 P. F. Duan, Y. G. Li, J. Jiang, T. Y. Wang and M. H. Liu, *Sci. China: Chem.*, 2011, **54**, 1051–1063.
38 P. F. Duan, Y. G. Li and M. H. Liu, *Sci. China: Chem.*, 2010, **53**, 432–437.
39 Y. G. Li, T. Y. Wang and M. H. Liu, *Soft Matter*, 2007, **3**, 1312–1317.
40 W. Yu, Y. G. Li, T. Y. Wang, M. H. Liu and Z. S. Li, *Acta Phys.–Chim. Sin.*, 2008, **24**, 1535–1539.
41 M. Takafuji, Y. Kira, H. Tsuji, S. Sawada, H. Hachisako and H. Ihara, *Tetrahedron*, 2007, **63**, 7489–7494.
42 Y. Kira, Y. Okazaki, T. Sawada, M. Takafuji and H. Ihara, *Amino Acids*, 2010, **39**, 587–597.
43 M. M. Green, M. P. Reidy, R. J. Johnson, G. Darling, D. J. Oleary and G. Willson, *J. Am. Chem. Soc.*, 1989, **111**, 6452–6454.
44 M. M. Green, N. C. Peterson, T. Sato, A. Teramoto, R. Cook and S. Lifson, *Science*, 1995, **268**, 1860–1866.
45 A. J. Wilson, J. van Gestel, R. P. Sijbesma and E. W. Meijer, *Chem. Commun.*, 2006, 4404–4406.
46 J. J. van Gorp, J. Vekemans and E. W. Meijer, *J. Am. Chem. Soc.*, 2002, **124**, 14759–14769.
47 M. J. Kim, B. G. Shin, J. J. Kim and D. Y. Kim, *J. Am. Chem. Soc.*, 2002, **124**, 3504–3505.
48 J. Yuan and M. H. Liu, *J. Am. Chem. Soc.*, 2003, **125**, 5051–5056.
49 D. K. Kondepudi, K. L. Bullock, J. A. Digits, J. K. Hall and J. M. Miller, *J. Am. Chem. Soc.*, 1993, **115**, 10211–10216.
50 Y. F. Qiu, P. L. Chen and M. H. Liu, *J. Am. Chem. Soc.*, 2010, **132**, 9644–9652.
51 J. M. Ribo, J. Crusats, F. Sagues, J. Claret and R. Rubires, *Science*, 2001, **292**, 2063–2066.
52 X. Huang, C. Li, S. G. Jiang, X. S. Wang, B. W. Zhang and M. H. Liu, *J. Am. Chem. Soc.*, 2004, **126**, 1322–1323.
53 S. Y. Zhang, S. Y. Yang, J. B. Lan, S. J. Yang and J. S. You, *Chem. Commun.*, 2008, 6170–6172.
54 J. H. Jung and S. Shinkai, in *Templates in Chemistry I*, ed. C. A. Schalley, F. Vogtle and K. H. Dotz, 2004, vol. 248, pp. 223–260.
55 H. Engelkamp, S. Middelbeek and R. J. M. Nolte, *Science*, 1999, **284**, 785–788.
56 C. F. Vannostrum, S. J. Picken and R. J. M. Nolte, *Angew. Chem., Int. Ed. Engl.*, 1994, **33**, 2173–2175.
57 C. L. Zhan, P. Gao and M. H. Liu, *Chem. Commun.*, 2005, 462–464.
58 J. J. Jiang, T. Y. Wang and M. H. Liu, *Chem. Commun.*, 2010, **46**, 7178–7180.
59 B. W. Messmore, P. A. Sukerkar and S. I. Stupp, *J. Am. Chem. Soc.*, 2005, **127**, 7992–7993.

Published on 25 April 2014. Downloaded by Michigan State University on 24/01/2016 09:49:48.

60 R. Oda, I. Huc, M. Schmutz, S. J. Candau and F. C. MacKintosh, *Nature*, 1999, **399**, 566–569.
61 X. F. Zhu, Y. G. Li, P. F. Duan and M. H. Liu, *Chem. – Eur. J.*, 2010, **16**, 8034–8040.
62 S. R. Nam, H. Y. Lee and J. I. Hong, *Chem. – Eur. J.*, 2008, **14**, 6040–6043.
63 A. Ajayaghosh, R. Varghese, S. Mahesh and V. K. Praveen, *Angew. Chem., Int. Ed.*, 2006, **45**, 7729–7732.
64 A. Ajayaghosh, C. Vijayakumar, R. Varghese and S. J. George, *Angew. Chem., Int. Ed.*, 2006, **45**, 456–460.
65 H. Cao, Q. Z. Yuan, X. F. Zhu, Y. P. Zhao and M. H. Liu, *Langmuir*, 2012, **28**, 15410–15417.
66 X. F. Wang, P. F. Duan and M. H. Liu, *Chem. Commun.*, 2012, **48**, 7501–7503.
67 M. Ikeda, R. Ochi, Y. Kurita, D. J. Pochan and I. Hamachi, *Chem. – Eur. J.*, 2012, **18**, 13091–13096.
68 Q. X. Jin, L. Zhang and M. H. Liu, *Chem. – Eur. J.*, 2013, **19**, 9234–9241.
69 M. Llusar and C. Sanchez, *Chem. Mater.*, 2008, **20**, 782–820.
70 E. D. Sone, E. R. Zubarev and S. I. Stupp, *Angew. Chem., Int. Ed.*, 2002, **41**, 1705–1709.
71 S. Kobayashi, N. Hamasaki, M. Suzuki, M. Kimura, H. Shirai and K. Hanabusa, *J. Am. Chem. Soc.*, 2002, **124**, 6550–6551.
72 A. Guerrero-Martinez, J. L. Alonso-Gomez, B. Auguie, M. M. Cid and L. M. Liz-Marzan, *Nano Today*, 2011, **6**, 381–400.
73 Y. G. Li and M. H. Liu, *Chem. Commun.*, 2008, 5571–5573.
74 D. D. Diaz, D. Kuhbeck and R. J. Koopmans, *Chem. Soc. Rev.*, 2011, **40**, 427–448.
75 J. J. D. de Jong, L. N. Lucas, R. M. Kellogg, J. H. van Esch and B. L. Feringa, *Science*, 2004, **304**, 278–281.
76 K. Murata, M. Aoki, T. Suzuki, T. Harada, H. Kawabata, T. Komori, F. Ohseto, K. Ueda and S. Shinkai, *J. Am. Chem. Soc.*, 1994, **116**, 6664–6676.
77 M. George and R. G. Weiss, *Chem. Mater.*, 2003, **15**, 2879–2888.
78 X. F. Wang, P. F. Duan and M. H. Liu, *Chem. – Eur. J.*, 2013, **19**, 16072–16079.
79 Y. Ji, G. C. Kuang, X. R. Jia, E. Q. Chen, B. B. Wang, W. S. Li, Y. Wei and J. Lei, *Chem. Commun.*, 2007, 4233–4235.
80 S. Wang, W. Shen, Y. L. Feng and H. Tian, *Chem. Commun.*, 2006, 1497–1499.
81 Y. G. Li, K. M. C. Wong, A. Y. Y. Tam, L. X. Wu and V. W. W. Yam, *Chem. – Eur. J.*, 2010, **16**, 8690–8698.
82 J. H. Kim, M. Seo, Y. J. Kim and S. Y. Kim, *Langmuir*, 2009, **25**, 1761–1766.
83 X. Chen, Z. Huang, S. Y. Chen, K. Li, X. Q. Yu and L. Pu, *J. Am. Chem. Soc.*, 2010, **132**, 7297–7299.
84 T. Tu, W. W. Fang, X. L. Bao, X. B. Li and K. H. Dotz, *Angew. Chem., Int. Ed.*, 2011, **50**, 6601–6605.
85 W. G. Miao, L. Zhang, X. F. Wang, H. Cao, Q. X. Jin and M. H. Liu, *Chem. – Eur. J.*, 2013, **19**, 3029–3036.
86 L. Qin, P. F. Duan, F. Xie, L. Zhang and M. H. Liu, *Chem. Commun.*, 2013, **49**, 10823–10825.
87 W. G. Miao, L. Zhang, X. F. Wang, L. Qin and M. H. Liu, *Langmuir*, 2013, **29**, 5435–5442.
88 Q. X. Jin, L. Zhang, X. F. Zhu, P. F. Duan and M. H. Liu, *Chem. – Eur. J.*, 2012, **18**, 4916–4922.
89 H. Cao, X. F. Zhu and M. H. Liu, *Angew. Chem., Int. Ed.*, 2013, **52**, 4122–4126.
90 H. Jintoku, M. Takafuji, R. Oda and H. Ihara, *Chem. Commun.*, 2012, **48**, 4881–4883.
91 B. Escuder, F. Rodriguez-Llansola and J. F. Miravet, *New J. Chem.*, 2010, **34**, 1044–1054.
92 F. Rodriguez-Llansola, J. F. Miravet and B. Escuder, *Chem. Commun.*, 2009, 7303–7305.
93 F. Rodriguez-Llansola, J. F. Miravet and B. Escuder, *Chem. – Eur. J.*, 2010, **16**, 8480–8486.
94 Q. X. Jin, L. Zhang, H. Cao, T. Y. Wang, X. F. Zhu, J. Jiang and M. H. Liu, *Langmuir*, 2011, **27**, 13847–13853.
95 A. Dawn, N. Fujita, S. Haraguchi, K. Sada and S. Shinkai, *Chem. Commun.*, 2009, 2100–2102.

 This journal is © The Royal Society of Chemistry 2014